Aalborg Universitet

AALBORG UNIVERSITY
DENMARK

Dynamic modeling, stability analysis and control of interconnected microgrids

A review

Naderi, Mobin; Khayat, Yousef; Shafiee, Qobad; Blaabjerg, Frede; Bevrani, Hassan

Dynamic modeling, stability analysis and control of interconnected microgrids: A review

Mobin Naderi [a], Yousef Khayat [a], Qobad Shafiee [a], Frede Blaabjerg [b,*], Hassan Bevrani [a]

[a] Smart/Micro Grids Research Center, University of Kurdistan, Sanandaj, POB: 416, Iran
[b] Department of Energy Technology, Aalborg University, Aalborg, DK, 9220, Denmark

GRAPHICAL ABSTRACT
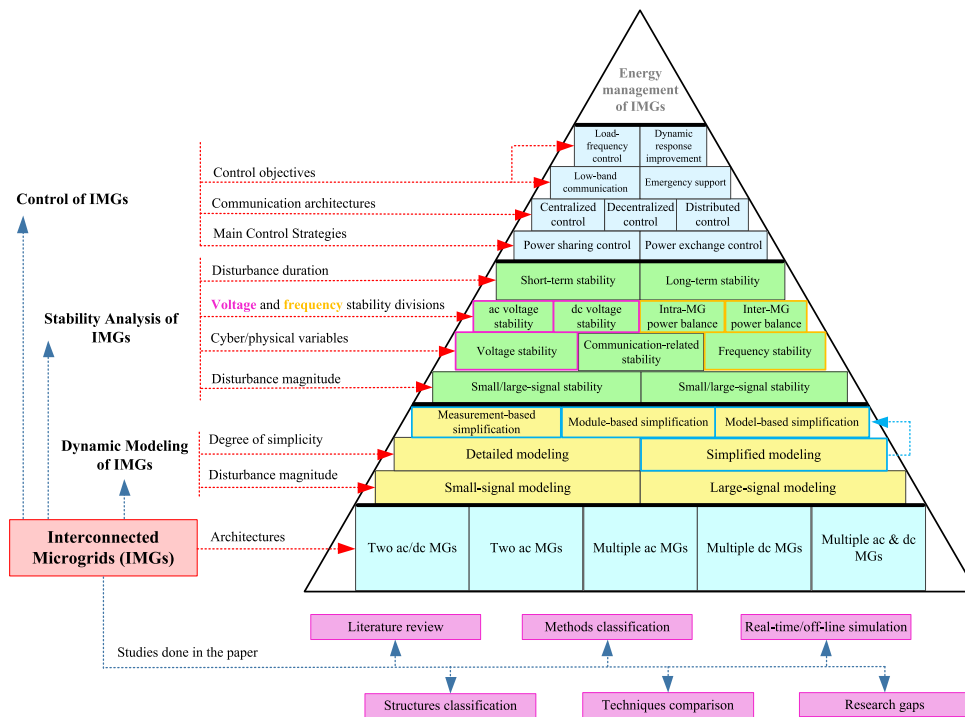
ARTICLE INFO

ABSTRACT

This paper reviews concepts of interconnected microgrids (IMGs) as well as compare and classify their modeling, stability analysis, and control methods. To develop benefits of isolated microgrids (MGs) such as reliability improvement and their renewable energy integration, they should be interconnected, share power, support the voltage/frequency of overloaded MGs, etc. Despite maximizing their benefits and decreasing weaknesses of isolated MGs, IMGs require maintaining stability in different operation modes and employing appropriate control methods. Moreover, a basic requirement for stability analysis and controller design is

* Corresponding author.
  E-mail addresses: m.naderi@uok.ac.ir (M. Naderi), y.khayat@uok.ac.ir (Y. Khayat), q.shafiee@uok.ac.ir (Q. Shafiee), fbl@et.aau.dk (F. Blaabjerg), bevrani@uok.ac.ir (H. Bevrani).

Power exchange control

system modeling. Since many articles have addressed these topics on IMGs from different views, a comparison is necessary. Therefore, IMG dynamic modeling methods are classified and their main features and challenges are discussed. Then, stability analysis and control methods of IMGs are reviewed and compared. The provided review is supported by conceptual diagrams, classification tables, off-line and real-time simulations using MATLAB and OPAL-RT simulator for comparison. Furthermore, a data set is provided to study fundamentals as well as research gaps, which are addressed for future works.

Nomenclature

Abbreviations:

BTBC	Back-to-back converter
CB	Circuit breaker
CRF	Common reference frame
DER	Distributed energy resource
IL	Interlinking line
ILD	Interlinking device
IMG (MG)	Interconnected microgrid (microgrid)
BTBC-2IMGs	Back-to-back converter-through two IMGs
CB-2IMGs	Circuit breaker-through two IMGs
MIMG	Multiple ac IMGs
MEB	Measurement-based (simplification technique)
MOB	Model-based (simplification technique)
MDB	Module-based (simplification technique)
PCC	Point of common coupling
PLL	Phase-locked loop
RTS	Real-time simulation
SOC	State of charge
SS	Static switch
TDS	Time-domain simulation
UIPC	Unified interphase power controller
VSC	Voltage source converters
VSG	Virtual synchronous generator

Variables:

$E_m(E_{PQ}^k)$	Inverter voltage of droop (PQ) control $DER_{m(k)}$
$i_l^m(i_{PQ,l}^k)$	Inverter current of droop (PQ) control $DER_{m(k)}$
$v_o^m(v_{PQ,o}^k)$	Filter voltage of droop (PQ) control $DER_{m(k)}$
$i_o^m(i_{PQ,o}^k)$	Filter current of droop (PQ) control $DER_{m(k)}$
v_{pcc}^n	PCC voltage of MG_n
i_{IL}^{nR}	Current of interlinking line between MG_n and MG_R
i_{lo}^n	Current of the load of MG_n
$\theta_m(\theta_{com})$	Voltage phase of DER_m (DER considered as CRF)
δ_m	Angle difference of DER_m's reference frame and CRF
δ_{PLL}^k	Angle difference of DER_k PLL's frame and CRF
$P_m(Q_m)$	Output active (reactive) powers of DER_m
$\omega_m(\omega_{com})$	Angular frequency of DER_m (DER considered as CRF)
X, U, Y	State, input, and output vectors in a state-space model
$i_{fc}^{i(j)}(v_{fc}^{i(j)})$	$VSC_{i(j)}$ output current (filter voltage)
$v_{dc}^{i(j)}$	$VSC_{i(j)}$ dc link voltage
$\theta_B^{i(j)}(\delta_B^{i(j)})$	$VSC_{i(j)}$ voltage phase (referred to the zone's CRF)
$m_d(m_q)$	Direct (quadrature) component of modulation signal

$Y_{PC}^{n,pin}$	Output vector of primary controller of leader DER in MG_n
$dq(DQ)$	Voltage/current direct and quadrature components (in CRF)

Constants, and Control Functions:

L_f^m, R_f^m	Inductance, and resistance of droop control DER_m filter
$L_{PQ,f}^k, R_{PQ,f}^k$	Inductance, and resistance of PQ control DER_k filter
$C_f^m(C_{PQ,f}^k)$	Capacitance of droop (PQ) control $DER_{m(k)}$ filter
$L_{li}^m(L_{PQ,li}^k)$	Inductance of droop (PQ) control $DER_{m(k)}$ line
$R_{li}^m(R_{PQ,li}^k)$	Resistance of droop (PQ) control $DER_{m(k)}$ line
$P_{ref}^k(Q_{ref}^k)$	Active (reactive) power reference of PQ control DER_k
$\omega_n(V_n^m)$	Nominal frequency (voltage) of MG_n (DER_m)
a_{mi}	mi'th array of intra-MG network adjacency matrix
$k_m^P(k_m^Q)$	$\omega - P(v - Q)$ droop gain of droop-based DER_m
$K_{SC}^{\omega-P}(s)$	Secondary controller of $\omega - P$ droop characteristic
$K_{SC}^{v-Q}(s)$	Secondary controller of $v - Q$ droop characteristic
$K_{VC}(K_{CC})$	Inner voltage (current) controller of DERs
T	Secondary controller time constant of leader DER

1. Introduction

Microgrids (MGs) are one of the main components of the future smart power grids, which are able to integrate nearby distributed energy resources (DERs) and loads at the distribution level in an efficient way. They also include several control loops and protection devices to achieve a stable and secure operation. Such a reconfiguration leads to independent management of MGs in grid-connected mode to maximize MG owners revenue, which can increase the energy value and thereby result in an economical operation. However, it should be in a coordinated operation with the upstream grid. MGs are able to be operated/controlled fully autonomous due to their DERs and energy storage systems, which can result in enhanced reliability, resilience and security [1]. Transition between grid-connected and isolated operating modes makes MG-oriented modern distribution grids more flexible than the conventional networks. The potential of more flexibility has been revealed once the idea of interconnected MGs (IMGs) was presented [2]. Active distribution networks can be reconfigured in the form of IMGs to have competitive markets and then a more economic energy management. In addition, remote autonomous MGs, which are geographically near each other, can be interlinked to benefit surplus of renewable energies. This new operating mode permits IMGs to exchange power to support frequency/voltage of critical MGs in emergencies as well as to supply power deficits in planned operations [3–6].

Optimal allocation of DERs, especially for renewable energy resources and energy storage systems, as well as optimal planning of MGs in future power grids are intensively affected by considering IMG operation, and should be rescheduled accordingly. Nevertheless, the proposed flexibility using IMG operation mode can improve schemes of optimal placement of DERs and optimal MG planning. Despite all
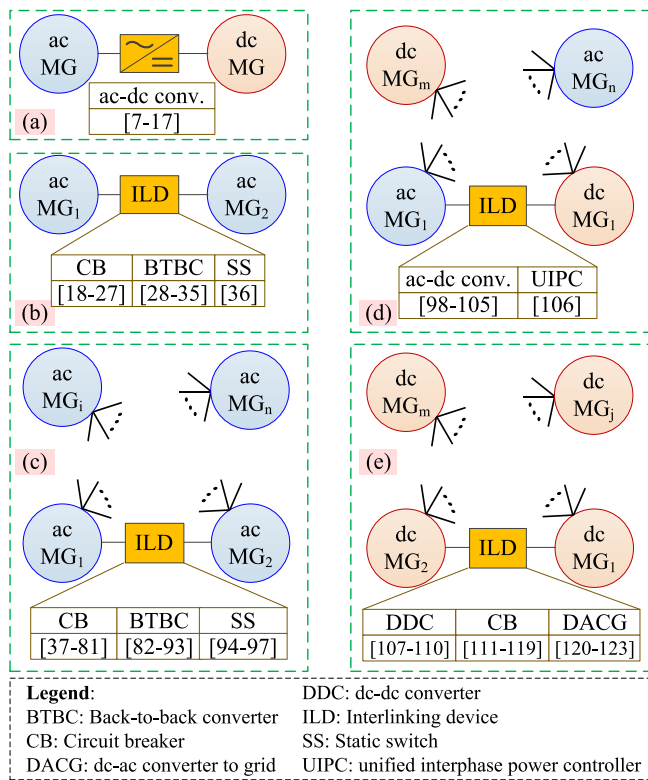
Fig. 1. General architectures of interconnected microgrids (IMGs): (a) hybrid ac/dc MGs, (b) two ac IMGs, (c) multiple ac IMGs, (d) multiple ac–dc IMGs, (e) multiple dc IMGs.

advantages of IMGs, basic studies on their stability and control as well as representing reliable and optimized control methods, and communication architectures are necessary in order to ensure a secure IMG operation. Modeling, stability analysis and control of IMGs have some similarities with other power systems, whether they are isolated/grid-connected MGs or multi-area power systems, which should be investigated. This paper aims to address these challenges by giving a comprehensive review.

1.1. Architectures of IMGs

Ac/dc MGs, ac/dc interlinking lines (ILs), interlinking devices (ILDs), power exchange control, as well as communication methods will lead to different IMG architectures [5,6]. Fig. 1 shows various structures of IMGs in terms of ILD and MG types. In Fig. 1(a), a simple schematic of hybrid ac/dc MGs is shown, where the ILD can only be a bidirectional dc–ac converter. Some important fields of hybrid ac/dc MG application are data center [7], telecommunication towers [8], electric vehicles and their charging stations [9,10], and shipboard MGs [11], where both ac and dc sources as well as ac and dc loads exist. Although the stability analysis of hybrid ac/dc MGs is less studied [12–14], different control issues and techniques of this architecture have been reviewed [8,15–17]. Therefore, this well-known architecture is not paid attention to details here except in the classifications.

Fig. 1(b) shows two ac IMGs, which are widely investigated due to the simple structure. According to the used ILD type, i.e. a circuit breaker (CB), a back-to-back converter (BTBC) or a static switch (SS), two ac IMGs can be categorized into three groups. The first group is named CB-2IMGs and consists of two MGs with the same voltage and frequency whether they are islanded or grid-connected [18–27]. The second is named BTBC-2IMGs, which uses BTBC to improve the

controllability of the power flow and supplementary objectives [28–35]. In the third group, an instantaneous SS is used, e.g. to support an overloaded MG [36].

In Fig. 1(c), multiple ac IMGs (MIMGs) are shown, which can be interlinked through CBs, BTBCs, or SSs. Researchers have done most contributions in MIMG due to the existing structure of the ac distribution networks and the discussed topics addressing their reconfiguration to improve stability, controllability, resilience, reliability, and power quality. The same structural classification is also considered for MIMG as CB-MIMG [37–81], BTBC-MIMG [82–93], and SS-MIMG [94–97]. Another architecture is multiple ac–dc IMGs as shown in Fig. 1(d). It can have different structures mostly dealing with various coordinative control of active power sharing/exchange [98–105], and their ILD topologies [101,102,104,106]. Generally, bidirectional dc–ac converters are used to establish the interconnections, but a UIPC is used in [106] to increase the flexibility of power exchange. In Fig. 1(e), the last architecture includes multiple dc MGs, which are interconnected to each other through dc–dc converters [107–110], and through dc CBs [111–119], as well as connected in parallel to the grid via dc–ac converters [120–123]. In this paper, the focus is on modeling, stability and control of two and multiple ac IMGs. Hence, other architectures are reviewed without more details.

Most addressed IMGs in the literature are grid-isolated, where individual voltage, frequency, and power sharing controls are required for each MG and coordination control is necessary for their interconnection. Nevertheless, there exist a few research papers that study grid-connected ac IMGs [83,85,99,124] and grid connected dc IMGs [120–123], where MGs are controlled to exchange a certain power with the main grid. In [99], the requirements and considerations for both grid-connected and islanded operation modes of CB-MIMGs are discussed. The application of the BTBC is demonstrated for grid-connected hybrid ac/dc MGs [124] and BTBC-MIMGs [85] using stability analysis to ensure a safe operation. In this paper, autonomous IMGs are in focus with different challenges of stability and control of voltage and frequency as well as global power sharing among the CB/SS-IMGs as well as power exchange among the BTBC-IMGs.

1.2. General view of IMG modeling

Dynamic modeling is the starting point of analyzing stability and synthesizing a large group of controllers, i.e. model-based controllers. According to the specific application, many modeling methods are already represented for modern DER-integrated power systems focusing on the generation side such as DER type e.g. combined heat and power systems [125], power converters [126], grid topology [127], load types [128], DER/MG control loops [1,129], and reduced-order modeling techniques [130–134]. However, IMGs require an individual modeling procedure using some known concepts of the common modeling methods as well as special considerations due to the large-scale aspect of IMGs including simplifications, which will depend on the application.

IMG Modeling is done considering a large-scale system including a large number of sub-systems, which needs developed methods with respect to that of a single MG with a limited number of modules. In fact, IMGs are more similar to multi-area conventional power systems in terms of structure and complexity for dynamic modeling with respect to isolated MGs. Moreover, each MG has a regional control, which requires it to be coordinated with regional controls of other MGs through a higher control level, i.e. a global control. For such large-scale power systems, simplified modeling methods are necessary in order to analyze dynamics and stability within an acceptable time interval, and also synthesize high-level controllers with desired performances, e.g. a frequency controller. Despite similarities of these two power systems, types of IMG modules and the corresponding dynamics are considerably different from those of conventional power systems, especially inverter-integrated DERs and renewable energy sources. Therefore, focusing

on IMGs modeling including both detailed and simplified types is important and differs from modeling of isolated MGs and conventional power systems.

Detailed models are investigated to identify the most significant participants, i.e. modules and parameters, in IMG stability and [73, 86,96,117]. On the other hand, simplified/reduced-order models are proposed for different applications including facilitating the stability analysis [51,65,67,68], analyzing stability of a designed controller [64, 72,116], and synthesizing the secondary controller of MGs for load-frequency control [21,23,70]. Note that dynamic modeling realized in short-term studies, e.g. minute-timescale, is of interest in this paper, but not the static modeling, e.g. fifteen-minute time-slots or larger, as it is more suitable for operation, energy management and planning investigations.

1.3. General view of IMG stability analysis

Due to the widespread system of IMGs and possible presence of several types of DERs, loads, converters and control loops, a stable operation is a challenge to obtain and ensure in all possible operational points. Inter-MG interactions that do not exist in isolated MGs are very important in terms of stability to be studied and identified. The modules cause such critical interactions and their parameters need to be precisely recognized. Although inter-area interactions and their corresponding dynamic modes have been studied for conventional power systems, their modules are different from those of modern IMGs due to existing a majority of renewable energies and storage systems in IMGs, and thus different results and observations are expected when studying IMGs interactions. Moreover, inter-inverter low-frequency dynamic modes have been recognized in autonomous MGs [135,136], which have a different source and different characteristics than inter-MG interactions.

In general, phenomena stability assessment, components influences on stability, stability analysis of designed controllers, and stability improvement are investigated as aggregated groups for different IMG architectures. Low-frequency oscillation in hybrid MGs [13], inter-MG dynamic modes [70], stability analysis of dc IMGs considering time-delay caused by wide-area measurements [37,113], frequency stability of CB-MIMG [60,61], and initial BTBC dc voltage in BTBC-MIMG [87] are studied as phenomena. Some others have focused on IMG stability assessment using eigenvalue analysis [12,14], participation matrix [64, 73], stability margin criteria [87,95], Lyapunov methods [51,117], and time-domain simulation (TDS) [13,27,39]. After designing the controllers, the IMG stability analysis is taken into account [110,116,118], and in some cases, stability improvement is a control objective to be realized [35,66,73]. The IMG stability is also improved by IMG clustering optimization and optimal placement of connection points among MGs [68,137].

1.4. General view of IMG control and optimization

Hierarchical control includes primary, secondary, and tertiary control layers [138], as well as a global control layer in a four-level control scheme [1]. Each control layer is responsible for different duties, e.g. MG stabilization is done in the primary layer and voltage/frequency restoration in the autonomous mode is accomplished in the secondary layer. Hierarchical control seems to be the best solution for multi-layer multi-objective control of MGs, especially in the isolated operation mode [1,138] due to existing classified control layers and communication infrastructures. This should be developed for IMGs considering challenges like power exchange/sharing during planned and emergency IMG operations as well as ancillary services. Although the primary control level is the same for isolated and interconnected MGs, the secondary and tertiary/global levels should be restructured to adapt the IMG control goals and requirements. The secondary control must also consider the communications among IMGs to realize global power sharing and voltage/frequency restoration. The tertiary control needs to be reconfigured to consider power exchanges in various IMG electricity markets and to achieve optimal energy/power management.

Several objectives have been followed by controlling IMGs. Preventing emergency conditions (mostly overload/over-generation) are taken into account [36,88,97,120]. The distribution network is reconfigured to form IMGs and improve network features, including reliability [46, 139], controllability [41], scalability and efficiency [107,139], availability and supply security [29,31], higher efficiency and lower reserve requirements [30], and cost minimization [25]. Different multi-level control approaches of power exchange among IMGs through power converters [84,110,123] and power sharing among synchronous IMGs through CBs and SSs [48,57,114,118] are presented to improve certain control indices. Similar control methods are investigated to optimize the power management and consider economic aspects [56,79,116], improve stability indices e.g. parameters margins [73], time-delay stability [37,116], power oscillation damping [93], low inertia [71], and dynamic stability [50,51,71], and to enhance communication factors, including communication burden decrease using event-triggered methods [45,75,76], time delays [100], cyber–physical security [42], and packet loss and communication failures [80,83]. The final research field is load-frequency control, where some have tried to use multi-area power system control/analysis methods for IMGs [21,23,33,48].

1.5. Contributions of the paper

Numerous valuable papers have been published to investigate dynamic modeling, stability analysis, and control challenges of IMGs for more than a decade. Therefore, it is natural to review, categorize and compare them from different aspects. Although there exist generally a few reviews related to MGs, their stability studies, and control approaches, contribution and objectives of this paper, which focus on ac IMGs, not individual MGs, are new.

Most relevant review papers deal with individual MGs and hybrid ac/dc MGs. For individual ac and dc MGs as well as hybrid ac/dc MGs, stability and control aspects [15], and control techniques [17] have been reviewed. Specifically for dc MGs, power sharing, voltage restoration and stabilization methods [140], architectures, applications and standardization [141] have already been reviewed. Furthermore for ac MGs, stability classification [142], demand side modeling and control [143], modeling and stability analysis of voltage source converter-dominated power systems [144], power sharing control strategies [145,146], harmonic modeling and stability analysis [147], grid-synchronization stability analysis [148], and secondary control architectures [149] have also been discussed. None of these review papers deals with dynamics and control of IMGs, which have different control loops, components, and consequently various dynamic interactions and stability challenges.

On the other hand, IMG systems and their issues have been reviewed more limited. IMG architectures and configurations have been of interest [5,6], which are categorized from several aspects, e.g. type of voltage and ILs. Moreover, general features of IMG architectures are discussed, e.g. reliability, scalability and protection [6]. In [150], although the main focus is on the distributed coordination control and optimization in MGs based on multi-agent systems, different applications in IMGs are also addressed. The most similar literature review [4] focuses on general aspects of IMGs including architecture, control, communication, and operation. However, it does not review the modeling and stability analysis of IMGs. Whereas, this paper presents a comprehensive review of dynamic modeling, stability analysis and control approaches of IMGs. The major contributions are given as below.

- Dynamic modeling, stability analysis and control techniques of IMGs are fully reviewed and compared from the viewpoint of a number of different technical aspects. Dynamic modeling methods are compared in terms of simplification type, order level of the

obtained model, method scalability, modeling technique, and software used for simulations. Stability analysis tools, general groups of studies, and important features of the corresponding literature are considered as technical aspects of stability analysis methods. Control techniques of IMGs are reviewed according to important features like control architecture, used communication bandwidth, control design method, validation method of controller performance, and main control objective. Graphical and tabular classifications are represented for all the three fields.

- Considerations and requirements of both detailed and simplified modeling methods of large-scale IMGs are represented for CB-IMGs and BTBC-IMGs. Furthermore, considerations to find open-loop and closed-loop models of IMGs are provided for different applications of stability analysis and control synthesis. Common methods for realizing interconnections among models of modules are compared in terms of computation burden as well as simplification methods of high-order IMG models are investigated from the modeling accuracy point of view.

- Eigenvalue analysis, sensitivity analysis, off-line and real-time simulation results are provided to improve the theoretical comparison of methods. As a review paper, useful links to the references are also provided for more simulation results, analysis and discussions, as well as experimental tests. Moreover, a data repository is provided including files for dynamic modeling, stability analysis, and off-line simulation of MGs as the main modules of IMGs, and IMGs themselves in [151].

- Main differences among modeling, stability and control of IMGs, individual MGs, and conventional multi-area power systems are discussed throughout the paper due to some similarities of these three groups of power systems. MGs and IMGs have generally similar types of DERs. On the other hand, IMGs and multi-area power systems have similar grid topologies and control architectures.

- In addition to a comprehensive literature review, research gaps and challenges in all the three fields, namely dynamic modeling, stability analysis, and control of IMGs are proposed for potential researchers to define and solve corresponding problems, and to improve applied methods and analyses for future works.

The rest of this paper is organized as follows. IMG dynamic modeling, concepts, classification, and methods are represented in Section 2. Stability analysis and assessment techniques are discussed in Section 3. Section 4 deals with control methods, their classification and comparison. In Section 5, the corresponding research gaps are addressed. Section 6 concludes the paper.

2. Dynamic modeling of interconnected microgrids

MG/IMG dynamics can be defined as changes and rate of changes of the phenomena related to MG/IMG control and operation. Accordingly, MG/IMG modeling is a mathematical equivalence in order to study dynamics of a specific phenomenon or a group of phenomena in a range of frequencies shown in Fig. 2. The phenomena can be classified into four groups in terms of change rate comprising very fast, fast/medium, slow and very slow.

Very slow dynamics belong to very long-term phenomena, which are approximately considered as longer than 1 hr. Power management and load forecasting in the MG layer and planned reconfiguration scheduling in the IMG layer are examples for very long-term phenomena. Slow dynamics are equivalent to long-term phenomena, which are considered as phenomena that take long between 1 min and 1 hr, i.e. dynamics with frequencies between the range 0.017 Hz to 2.78×10^{-4} Hz. Demand response and energy management within MGs and energy exchange management between IMGs are good instances for this category. Fast and medium dynamics are assumed with frequencies between 1 Hz and 0.017 Hz, which are equivalent to the short term and medium phenomena with an almost fast occurrence time from 1
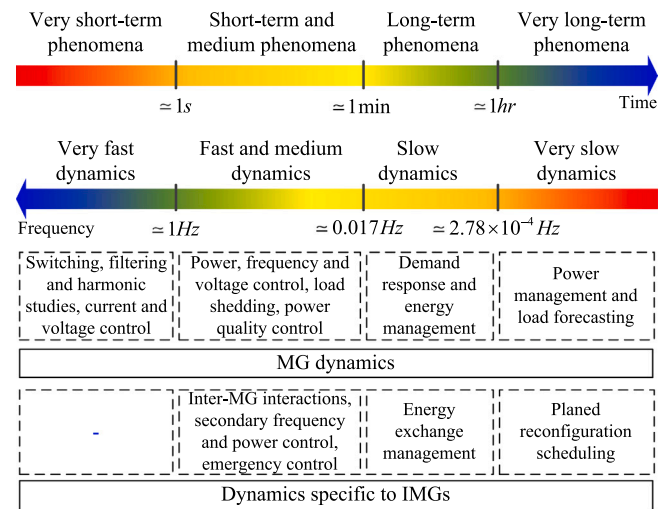

Fig. 2. MG and IMG phenomena classification based on frequency ranges and correlated time durations.

s to utmost 1 min. Common control processes of the power, frequency and voltage as well as load shedding and power quality control are fast/medium phenomena in MGs and Inter-MG interactions [1], secondary frequency and power controls, and emergency control of IMGs are fast/medium phenomena related to IMGs.

The final group includes very short-term phenomena, which happen less than 1 s, i.e. very fast dynamics. Dynamics of power converter switching, filtering and harmonic control loops as well as a part of dynamic modes of current and voltage control loops can be considered as very fast dynamics in MG studies. However, interactions of IMGs and their control loops do not include very fast dynamics due to the incremental bandwidth considered in designing the control loops of MGs and IMGs from the innermost loop to the outermost loop.

For each frequency range, different types of modeling methods with their requirements are needed to model the corresponding dynamics, which in turn can be categorized into detailed/full-order and simplified/reduced-order modeling types. A detailed modeling method leads to a large range of frequencies while simplified models focus on a special frequency range, e.g. low frequencies [70]. In Fig. 3, two conceptual diagrams clearly show the differences of detailed and simplified modeling methods. Generally, in studying a specific phenomena or certain application, some dynamics are not modeled or will be removed after modeling to find a simplified model. On the other hand, in order to study a specific frequency range of dynamics or a multi time-scale phenomena, detailed modeling is required, which results in modeling a wide range of frequencies.

Another classification presented in Fig. 3, is based on the linear/nonlinear behavior of MG/IMG dynamics. Linear-dynamic modules can only be modeled using small-signal modeling methods including state-space representation and transfer function. Nevertheless, according to the requirement and application, both small-signal and large-signal modeling methods are able to be used for modeling nonlinear-dynamic modules. Common methods of large-signal modeling are nonlinear equations governing the module dynamics and block diagram-based simulations using modeling softwares, e.g. MATLAB and PSCAD/EMTDC. In fact, block diagram-based simulations are easy represented visual forms to implement linear and nonlinear equations, which model control and electrical circuit fundamentals. Simulink and SimPowerSystems are MATLAB environments for dynamic modeling of control and power systems using block diagram-based simulations, whereas Editor environment of MATLAB can be used for dynamic modeling via implementing nonlinear equations.

Fig. 3 shows some corresponding literatures of dynamic IMG modeling, whereas Table 1 shows a comprehensive literature review on IMG
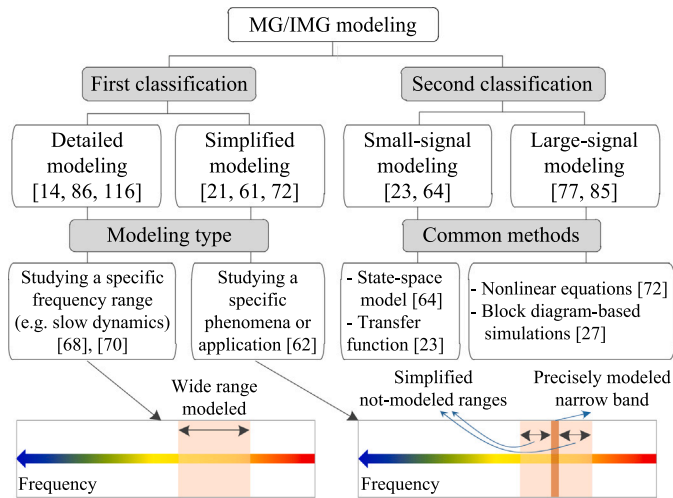
Fig. 3. MG/IMG modeling classification including detailed, simplified, small-signal, and large-signal categories.

modeling, where the most-important features are determined. Useful comparisons can be seen in each column. Modeling type discussed earlier, model order level in four groups including very low (VL), low (L), medium (M), and high (H), the subcategories of simplified modeling type, the scalability of the addressed methods, and the methods and tools used in modeling are taken into consideration.

Transfer function (TF) is a simple modeling method for (very) low order linear models, which can be extended as TF matrix for multivariable systems. However, it is less flexible than state-space representation (SSR) and thus unsuitable for large-scale IMG modeling. Block diagram is not an independent analytical tool, but it can be useful for software-defined modeling, and facilitating SSR and TF methods. Differential equations (DEs) are a more general modeling tool than TF and SSR, which can model both linear and nonlinear dynamics. Static equations (SEs) are an approximation of non-important dynamics to be neglected in module-based (MDB) and measurement-based (MEB) models. However, singular perturbation (SP) is a similar analytical method for model-based (MOB) simplifications. Prony analysis (PA) is used in MEB modeling to identify dynamic modes of a waveform. Kron reduction (KR) is only applicable in electrical circuit model reduction to remove interior nodes and preserve dominant nodes. Another powerful tool for this objective is Krylov subspace theory (KST), which is based on space projection.

The last column of Table 1 represents simulation and modeling softwares used in the literature. Generally, the simulation softwares of power systems are license-based including MATLAB, PSCAD/EMTDC, DIgSILENT Power Factory, PLECS, and DSA. However, there are different licenses for commercial uses, research projects and educational purposes in universities and academic institutions, and personal use of students. DIgSILENT has a thesis-based license, which can add just the required features for a non-sponsored bachelor/master/PhD thesis in a limited time with a lower price. There are also some free productions. PSCAD/EMTDC has a free version with limited network size, i.e. maximum 15 electrical nodes. It is useful for MG and some IMG studies, where the electrical networks are small. The control components are not limited. MATLAB has a free 30-day trial version. PLECS, which is a simple environment for power electronics and power systems simulations, has a 90-day free trial license. Although these softwares execute off-line simulations, OPAL-RT, RTDS, and dSPACE are real-time simulators for hardware-in-loop simulations. In addition to real-time simulations, they can be used for experimental tests, where the control desk, power components, or both are implemented in a laboratory.

Basically MATLAB/Simulink, MATLAB/SimPowerSystems, PSCAD, DIgSILENT, PLECS, DSA, OPAL-RT, RTDS, and dSPACE are environments for block diagram-based modeling and simulations. However, complementary programming can be done in some softwares. The type of softwares are generally not mentioned for Linear modeling in references shown in Table 1 for small-signal stability analysis. Some possible and common softwares for programming are C, C++, Python, MATLAB/Editor, and MAPLE. In [95,96], MATLAB/Editor is addressed for modeling and stability analysis. In [38,86], Robust Control Toolbox (RCT), in [61], Power System Toolbox (PST), and in [65], COntinous Reachability Analyzer (CORA) toolbox of MATLAB are used for modeling and stability analysis. MATLAB and MAPLE, which are softwares with possibility of programming, can be used using a license, however individual programming environments are generally free, e.g. Python, C, C++.

2.1. Detailed modeling methods

In order to provide a detailed model of IMGs, the subsystems/modules should be separately modeled and then their interconnections including power lines and control signals are considered. Control signals can be realized by physical cabling, communicating data, or their combination. The main modules constructing IMGs are MGs, ILDs, ILs, and their controllers. Modeling of modules is often done using SSR. IMG interconnections can be modeled by precisely considering the connections among inputs and outputs of the module models. Although the basic analytical method of several equation substitutions is addressed in the literature [57,64,73,94] for IMG interconnection modeling, the analytical–numerical methods [38,70,86] are more favored due to reducing the computational burden of modeling numerous nested IMG interconnections and consequently low computation time.

2.1.1. MG module modeling

Fig. 4 shows a block diagram of a typical ac MG in an IMG structure used to find the detailed model for the purpose of dynamic stability and control studies. The details of the power components including DER LC filters, coupling lines, ILs and loads are shown in Fig. 4(a). Both droop-based (grid forming) and PQ-controlled (grid feeding) DERs are included, where the control components are indicated in Figs. 4(b) and 4(c).

Droop-based DERs are responsible for MG voltage and frequency control and stabilization as well as power sharing to preserve load-generation balance after disturbances and to prevent current circulating among DERs. The control strategy of each droop-based DER is formed from a current controller, a voltage controller, a droop-based primary control layer and a secondary control layer. Inner current and voltage controllers regulate output current of the DER and the voltage of its output filter. The primary control stabilizes voltage and frequency by appropriate references and shares the load power among DERs without communication according to their rated powers. The secondary control basically does complementary actions for the primary control including voltage and frequency restoration to their nominal values and power sharing improvement generally using communication. The required signals from a higher level IL power controller can also be seen in Fig. 4(b), which are added to the secondary control loop.

On the other hand, the PQ-controlled DERs try to inject maximum powers of renewable energies to the grid by controlling output active and reactive powers. A current controller and a current reference generator from the active and reactive power references can cope with this objective. Moreover, a phase-locked loop (PLL) is required to synchronize the generated DER voltage with the grid voltage. As shown in Fig. 4(c), PQ-controlled DERs do not participate in voltage and frequency control as well as in higher control layers related to IMGs. The variables and coefficients are specified in [70,86]. Each MG can also be considered as a large-scale system especially when it

Table 1
IMG dynamic modeling literature review.

Reference	Modeling type	Order level	Simplifying type	Scalability	Modeling method	Simulationsoftware
[20,21,23]	Simp.	VL	MDB	Low	TF	MATLAB/Simulink
[60]	Simp.	VL	MDB	High	TF, PA	Not mentioned
[61]	Simp.	VL	MDB	High	TF, PA	MATLAB/PST, DSA, PLECS, MAPLE
[152]	Simp.	M	MOB	High	KST	MATLAB/SimPowerSystems
[14]	Detailed	H	–	L,M	SSR	PSCAD/EMTDC
[116]	Detailed	H	–	L,M	SSR	MATLAB/Simulink, OPAL-RT/RT-LAB
[117]	Detailed	H	–	L,M	SSR	dSPACE
[64]	Detailed	H	–	L,M	SSR	MATLAB/Simulink
[95,96]	Detailed	H	–	L,M	SSR	MATLAB/Editor, PSCAD/EMTDC
[73]	Simp.	M	MDB	High	SSR	PSCAD/EMTDC
[77]	Detailed	H	–	Low	RTDS BD	RTDS
[72]	Simp.	L	MDB	Medium	DF, SSR	MATLAB/SimPowerSystems
[85]	Simp.	L	MDB	Medium	DF, SSR	MATLAB/Simulink, PSCAD
[65]	Simp.	VL	MDB	Medium	TF	MATLAB/CORA
[153]	Simp.	VL	MEB	High	SE	OPAL-RT
[68]	Simp.	M	MOB	Low	SSR, SP	MATLAB/Simulink
[62]	Simp.	M	MDB	High	Agg., KR	MATLAB/SimPowerSystems
[27]	Simp.	M	MDB	Low	Sim. BD	DIgSILENT
[57]	Simp.	M	MDB	High	SSR	PSCAD/EMTDC
[51,59,69]	Simp.	VL	MDB	High	SSR, SP	Not mentioned
[38,86]	Detailed	H	–	High	SSR	MATLAB/RCT, OPAL-RT
[70]	Simp.	VL	MOB, MDB	High	Agg., TF	MATLAB/RCT, MATLAB/Simulink

L: low, M: medium, H: high, VL: very low, MDB: module-based, MOB: model-based, MEB: measurement-based, TF: transfer function, PA: Prony analysis, KST: Krylov subspace theory, BD: block diagram, SSR: state-space representation, DF: differential equations, SE: static equations, SP: singular perturbation, Agg.: aggregation, KR: Kron reduction, PST: Power System Toolbox, DSA: Dynamic Security Assessment, RCT: Robust Control Toolbox, CORA: COntinous Reachability Analyzer.

includes a large various number of DERs and loads, which should be modeled and then their interconnections must be considered.

Modeling of the power components, inner control loops and primary control are just considered in most of the literature [14,86,95,96,117], which are usually modeled using a state-space representation (see Table 1). Others have included the secondary control in the detailed model [64,116,117]. The secondary control structure shown in Fig. 4 is a distributed consensus one, which is reviewed and discussed in [149] and mostly used in the IMG modeling and control by considering two cyber networks for Inter-MG and Intra-MG communications [57,73,94, 116,117].

The IL controller, which its synthesis and analysis are the state of the art, may has different structures to analyze power exchange [64], control IL current [94], and share IMG power [57]. Hence, several models can be considered, e.g. BTBC is used to control power exchange [85, 86], where models of its control and power components need to be added in the modeling. By contrast, a distributed power sharing control is usually used in CB-IMGs, where the IL power controller will be a part of the secondary controller of each MG [38,64] and will be modeled there.

Fig. 5 shows the interconnections among sub-modules of the general MG module represented in Fig. 4. The main sub-modules can be considered in three groups, including sub-modules of the MG power network, droop-based DERs, and PQ-controlled DERs. The MG power network includes dynamic models of DER coupling lines and MG loads as well as static equation(s) of the point of common coupling (PCC) voltage(s) and required transformations from the CRF to the individual reference frame shown by DQ/dq blocks in Fig. 5. Sub-modules of droop-based DERs consist of dynamic models of the voltage source converter (VSC), LC filter, current controller, voltage controller, primary control, and secondary control. Sub-modules of PQ-controlled DERs include dynamic models of the VSC, output LC filter, current controller and PLL. Both droop-based and PQ-controlled DERs require transformations from the individual reference frames to the CRF shown by dq/DQ blocks in Fig. 5 [127]. The models of sub-modules except the secondary controller can be found in [86,127]. The secondary controller model is intensively affected by the communication architecture and control objectives. For instance, a typical pinning consensus-based distributed secondary controller, which follows power sharing and voltage/frequency regulation control objectives, is modeled and details of the matrices and vectors are presented in [38,72,79].

Following electrical, control, and communication laws, using mathematical relationships and employing numerical calculations, each AC MG with any number of DERs, lines and loads can be represented via a state-space model as follows:

$$\dot{X}_{MG}^n = A_{MG}^n X_{MG}^n + B_{MG}^n U_{MG}^n,$$
$$Y_{MG}^n = C_{MG}^n X_{MG}^n + D_{MG}^n U_{MG}^n, \qquad (1)$$

where the state vector can be organized as

$$X_{MG}^n = [X_{DER}^{DB1} \quad \cdots \quad \overbrace{X_{SC}^m, X_{PC}^m, X_{VC}^m, X_{CC}^m, X_{PD}^m}^{X_{DER}^{DB,m}} \quad X_{DER}^{PQ1}$$
$$\cdots \quad \overbrace{X_{PLL}^k, X_{CC}^k, X_{PD}^k}^{X_{DER}^{PQ,k}} \quad X_{CL}^1 \quad \cdots \quad X_{CL}^{m+k} \quad X_{ML}], \qquad (2)$$
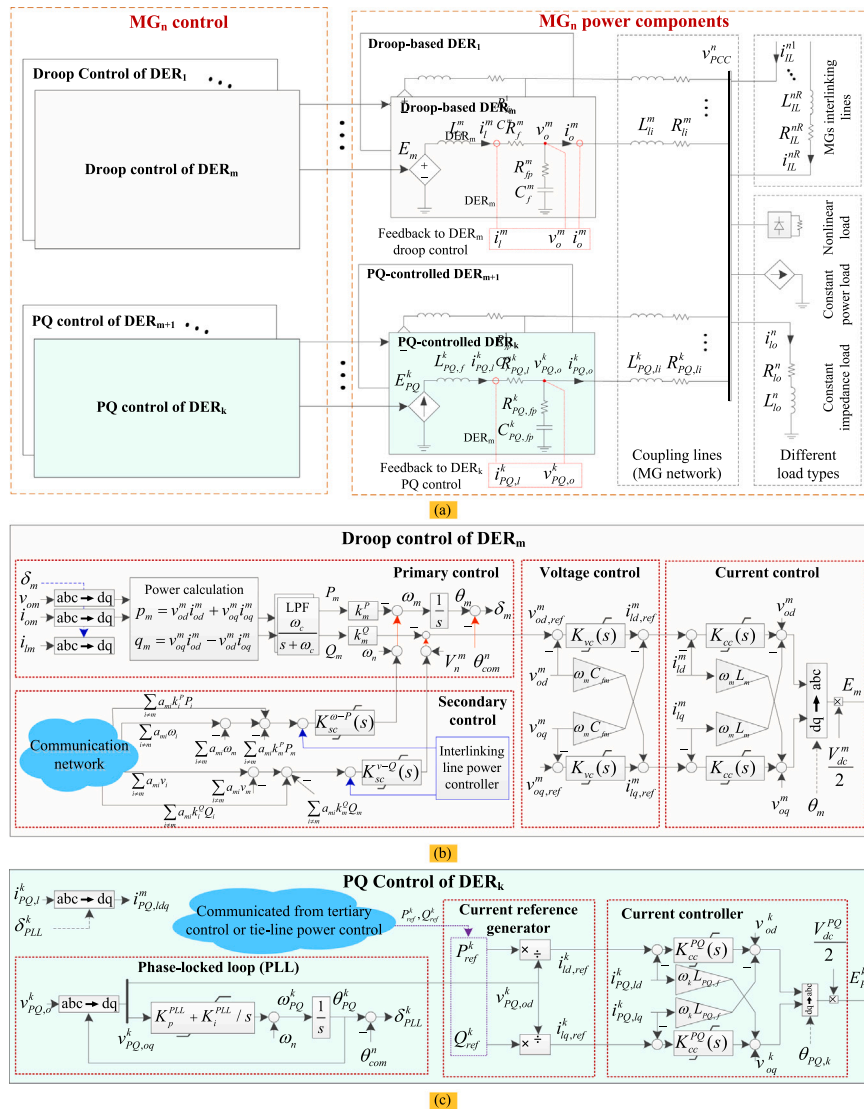
Fig. 4. Block diagram of a typical ac microgrid in an IMG structure used to achieve the detailed model for the purpose of dynamic stability and control: (a) model of MG power components comprising voltage and current sources, LC filters, DER coupling lines, loads, and IMG interconnecting lines, (b) droop control of DER$_m$, (c) PQ control of DER$_k$.
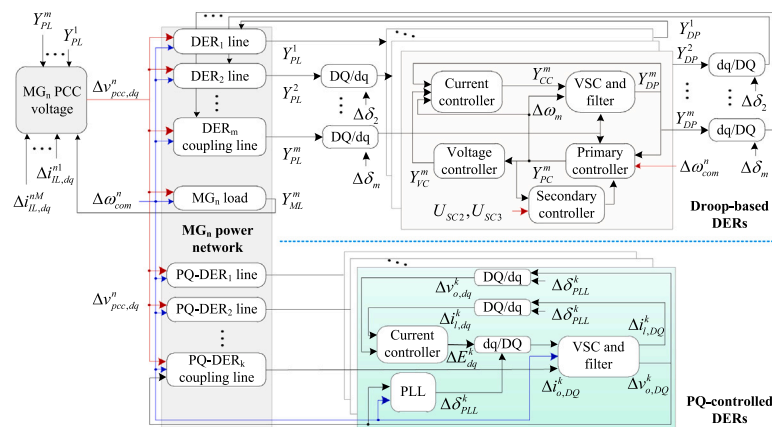
Fig. 5. Internal MG connections to find the overall state-space model of the MG module represented in Fig. 4.
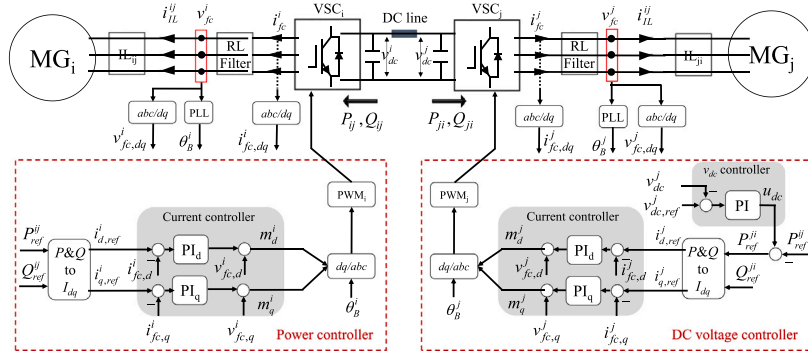
Fig. 6. Details of modeling BTBC modules including power components of ac and dc sides between IMGs, and power and dc voltage control loops [85,86,154].

and it consists of $15m + 10k + 2$ state variables for the MG structure shown in Fig. 4, where m is the number of droop-based DERs and k is the number of PQ-controlled DERs. Interlinking line currents to MG_n are as the inputs i.e. $U_{MG}^n = [i_{IL,dq}^{n1} \ldots i_{IL,dq}^{nM}]^T$ and the MG_n output can be considered as $Y_{MG}^n = [\Delta\omega_{com}^n \ \Delta v_{pcc,dq}^n \ Y_{SC}^{n,pin}]^T$.

2.1.2. CB module modeling

CBs and instantaneous SSs have fast responses in the range of microseconds and milliseconds. Therefore, the CB/SS dynamic model in CB-IMGs/SS-IMGs modeling is neglected due to its much faster dynamics than the studied MG/IMG dynamics explained in Fig. 2.

2.1.3. BTBC module modeling

As shown in Fig. 6 a BTBC is usually controlled by two controllers, i.e. power controller and dc voltage controller to exchange power between two ac IMGs. The power controller receives the active and reactive power references from the IMG tertiary/global controller to exchange scheduled powers by controlling the VSC_i. On the other hand, the dc voltage controller stabilizes the dc link voltage by controlling the VSC_j. In addition, two PLLs are required for the VSCs to synchronize them with the MGs.

Ac and dc sides of each VSC is modeled by a two-port, in which the ac side is modeled using a dependent voltage source connected to the filter components, and the dc side is modeled using a dependent current source connected to the dc link capacitors and dc line model [154,155]. Then, modeling is straightforward from circuit laws to a state-space representation. The controllers can also be modeled by considering each integrator output as a state variable. Note that all these modules, i.e. power and dc voltage controllers, PLLs, and dc and ac power components are independently modeled using state-space representations, where the details is represented in [85,86,154]. For the ease of modeling, interconnections among the modules is done in the next step, generally like interconnecting IMG modules, which is explained in the next interconnection sections.

Fig. 7 shows all BTBC interconnections among power and control sections, which are necessary to find its state-space model like (1) [86]. The control section of the $BTBC_{ij}$ includes the dynamic models of the PLLs, power controller and dc voltage controller as shown in Fig. 7. The BTBC power components comprise averaging static models of VSCs, and dynamic models of RL filters at the ac sides and dc link capacitors and dc lines at the dc side. Note that required Park and Park inverse transformations are shown in Fig. 6 and some other transformations to/from the CRF required for detailed modeling of BTBCs can be found in [86], which all can be modeled using static equations. Finally, the state vector X_B^{ij} of the $BTBC_{ij}$ is a 21×1 vector as $X_B^{ij} = [X_{BP}^{ij} \ X_{Bpc}^i \ X_{Bcc}^j \ X_{DVC}^j \ X_{PLL}^i \ X_{PLL}^j]^T$, and the input and output vectors are as $U_B^{ij} = [\Delta v_{pcc,dq}^i \ \Delta i_{IL,dq}^{ij} \ \Delta v_{pcc,dq}^j \ \Delta i_{IL,dq}^{ji} \ \Delta\omega_{com}^i \ \Delta\omega_{com}^j]^T$ and $Y_B^{ij} = \left[\Delta v_{fc,dq}^i \ \Delta v_{fc,dq}^j \ \Delta v_{dc}^j \ \Delta\delta_B^i \ \Delta\delta_B^j\right]^T$. The matrices have been found in [86].
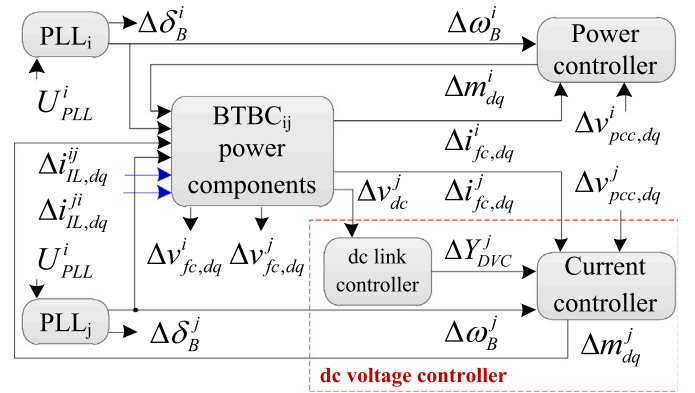

Fig. 7. Interconnections among the $BTBC_{ij}$ power and control modules [86].

2.1.4. Interlinking line module modeling

In low/medium voltage IMGs, the length of ILs is usually low/medium. Hence, they are modeled as series RL branches like DER coupling lines within MGs. The considerations of the IL current direction and the reference frame in the modeling process, are accessible for CB-IMGs [38,96] and BTBC-IMGs [86]. The state-space representation for IL_{ij}, i.e. between MG_i and MG_j, can be given as follows:

$$\dot{X}_{IL}^{ij} = A_{IL}^{ij} X_{IL}^{ij} + B_{ILM}^{ij} U_{ILM}^{ij} + B_{ILB}^{ij} U_{ILB}^{ij},$$
$$Y_{IL}^{ij} = C_{IL}^{ij} X_{IL}^{ij}, \tag{3}$$

where $X_{IL}^{ij} = Y_{IL}^{ij} = \Delta i_{IL,dq}^{ij}, U_{ILB}^{ij} = \Delta v_{fc}^{ij}, U_{ILM}^{ij} = [\Delta v_{pcc,dq}^i \ \Delta\omega_{com}^i]^T$, and the matrices are addressed in [86].

2.1.5. CB-IMG interconnections

Fig. 8 shows the details of interconnections among CB-IMGs with a common pinning consensus-based distributed secondary control architecture [45,46,57,72,73,76,79]. Each MG is divided into two sets of components, i.e. control components and power components. A CRF should be considered for sub-models stated in the individual reference frames to be transformed in it [38]. The CRF zone comprises all ILs as well as power components of the MGs. In fact, all these components lack an individual frequency reference. The PCC voltage of each MG, e.g. $\Delta v_{pcc,dq}^n$ for MG_n, is as the input of the state-space models of the connected ILs, e.g. IL_{nl} between MG_n and MG_l. Inversely, the current of each IL is as the input to the dynamic model of connected MGs, e.g. ΔY_{IL}^{nl} for MG_n and MG_l. Another interconnection among IMGs belongs to the communication used to exchange the leader DERs information including voltage, frequency, and active and reactive output powers among them. All the required information of each MG for communication is obtained from the output of the state-space model of each leader DER, e.g. $Y_{PC}^{n,pin}$ of $DER_{n,pin}$ in MG_n.
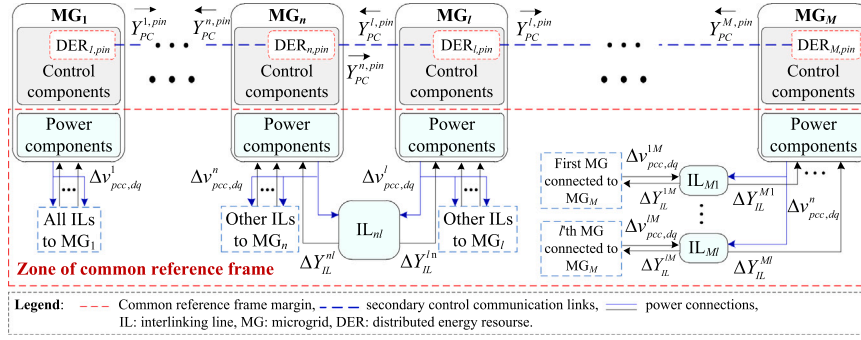
Fig. 8. Comprehensive interconnections among CB-IMGs through ILs including all inputs and outputs of the main modules [38].
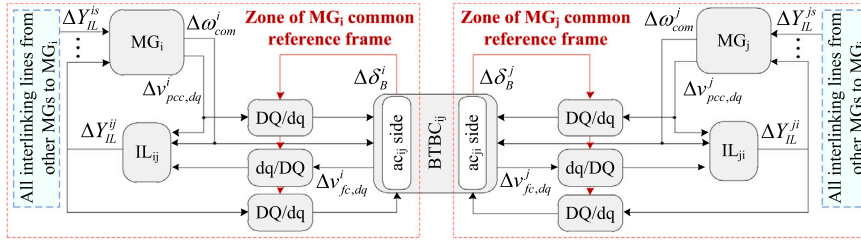

Fig. 9. Comprehensive interconnections of BTBC-IMGs focusing on MG_i and MG_j connected through IL_{ij}, IL_{ji} and $BTBC_{ij}$ [86].

2.1.6. BTBC-IMG interconnections

Fig. 9 shows BTBC-IMGs interconnections focusing on the interconnection between MG_i and MG_j including $BTBC_{ij}$, IL_{ij}, IL_{ji} [86]. In BTBC-IMGs due to frequency independence, MGs have individual CRFs, where their functional zones can be seen. Dynamic models of all ILs and BTBC AC sides connected to each MG should be stated in its CRF. Therefore, CRF to individual reference frames, and inverse transformations, i.e. DQ/dq and dq/DQ [86,127], are used for power interconnections between the MG/IL and the BTBC. In this regard, the common frequency, e.g. $\Delta\omega^i_{com}$ in MG_i zone, is used in the related module models. Typically, the PCC voltage of MG_i, $\Delta v^i_{pcc,dq}$, is delivered to IL_{ij} directly and to the ac_{ij} side through the MG_i CRF to the individual $BTBC_{ij}$ reference frame. The output current of IL_{ij}, ΔY^{ij}_{IL}, is also used directly in the MG_i model and after the same transformation in the $BTBC_{ij}$ model as an input. The last modeling interconnection is using the output voltage of the BTBC RL filter as an input to the IL after transforming from the individual BTBC reference frame to the MG CRF, e.g. using $\Delta v^i_{fc,dq}$ of $BTBC_{ij}$ in the state-space model of the IL_{ij}.

In BTBC-IMGs, the BTBCs are in charge of power exchanges in a coordinated manner with MGs productions, which is realized in the tertiary/global control layer. Hence, communication links among IMGs in the secondary control level are not dominant unlike CB-IMGs. Due to this reason as well as existing individual CRFs, the overall model of BTBC-IMGs has less complexity than that of CB-IMGs.

2.1.7. Overall IMG modeling

In general and for any types of IMGs, if a state-space representation is used for linear/linearized IMG modeling, the models (4) and (5) can be found. Model (4) is a free-motion closed-loop type, which is useful for stability/dynamics analysis of the overall system including power and control parts. The state vector X^{cl}_{IMG} is addressed for different IMG structures with various control architectures [14,64,95,96,116,117]. The exact form of the state matrix A^{cl}_{IMG} is hard to be find. However, its general form is presented in some literature for different control strategies of CB/SS-IMGs [14,38,96]. Moreover, a numerical method is represented to facilitate its calculation for both CB-IMGs and BTBC-IMGs [38,86].

$$\dot{X}^{cl}_{IMG} = A^{cl}_{IMG}X^{cl}_{IMG}, \tag{4}$$

Model (5) is an open-loop model, which can consider a desired control input and synthesize the corresponding controller, e.g. the IL power controller. X^{ol}_{IMG}, U^{ol}_{IMG}, and Y^{ol}_{IMG} are the state, input, and output vectors, respectively and A^{ol}_{IMG}, B^{ol}_{IMG}, C^{ol}_{IMG}, and D^{ol}_{IMG} are the well-known matrices, which should be calculated for different models. This model is not taken into account in the literature.

$$\dot{X}^{ol}_{IMG} = A^{ol}_{IMG}X^{ol}_{IMG} + B^{ol}_{IMG}U^{ol}_{IMG}, \tag{5a}$$

$$Y^{ol}_{IMG} = C^{ol}_{IMG}X^{ol}_{IMG} + D^{ol}_{IMG}U^{ol}_{IMG}. \tag{5b}$$

2.2. Comparison study: Interconnection and substitution modeling methods

In each type of IMGs, the interconnections among the dynamic models of the IMG modules can be realized in two general methods, namely substitution and interconnection methods. The substitution method has been used in most literatures, e.g. [57,64,68,73], which needs many substitutions of equations to obtain interconnections between models of modules. On the other hand, the interconnection method uses useful functions of Robust Control Toolbox to numerically realize interconnections in MATLAB/Editor [38,86]. The second is much simpler in calculation due to computing all electrical and control connections between individual modules employing MATLAB functions and without substituting equations in each other, which is a time-consuming manual process.

The substitution method is well-known, and mathematics is its basis. Required steps to apply the interconnection method are already explained [86]. Here, these two methods are compared in terms of computation burden/time for the case of BTBC-IMGs. When the substitution method is used for finding each MG model, the number of substituting can be found according to Fig. 5 and the output arrows from the blocks. For instance, the PCC voltage equation should be substituted in the line equation for all m lines and in the load equation for the load, which are totally $m+1$ substitutions. Considering m droop-based DERs and without PQ-controlled DERs, one can find all required manual substitutions as $12m+1$ for modeling a typical MG, which can be expressed as 13 when the similar substitutions are just considered as 1 substitution, i.e. $m=1$. The substitution process should be similarly used for BTBCs using Fig. 7 that leads to 24 substitutions for each BTBC. However, required ones are reduced to 13 by neglecting similar substitutions.

Table 2
Comparison of the substitution method [57,64,73] and the interconnection [38,86] method.

Modeling method	Possible manual error	Studied system	Number of substitution /input_to	Manual calculation time (min)
Substitution	Module modeling and substituting	IMG$_1$	291	1164
		IMG$_2$	676	2704
Interconnection	Module modeling and input specifying	IMG$_1$	157	157
		IMG$_2$	366	366

According to Fig. 9, for each interconnection between two MGs, 20 substitutions (10 by neglecting the similar ones) are required. For n different autonomous MGs with k BTBCs among them, totally $\sum_{i=1}^{n}(12m_i + 1) + 44k$ substitutions (36 by neglecting the similar ones) are required to find the BTBC-IMG model using the substitution method. This manual calculation causes a high calculation burden and requires much time. Nevertheless, in the interconnection method, the large number of substitutions are performed numerically with a low manual calculation burden only for specifying inputs of each module contributing in the interconnections shown in Figs. 5, 7, and 9. In other words, the calculation time/burden of the interconnection method can be determined as determining the inputs of modules using *input_to* function in MATLAB/Editor. The number of determining input vectors is equal to the number of modules to be interconnected. Therefore, It can be easily calculated for BTBC-IMGs as $\sum_{i=1}^{n}(7m_i + 2) + 20k$.

The calculation burden/error comparison is shown in Table 2 for the common substitution method [57,64,73] and the interconnection method [38,86] in two sample IMGs. In this comparison study, IMG$_1$ is formed by three interconnected MGs through three BTBCs, where MG$_1$ has three DERs, MG$_2$ has four DERs, and MG$_3$ has six DERs. IMG$_2$ is formed from eight interconnected MGs through seven BTBCs, where each one of MG$_1$-MG$_3$ has two DERs, each one of MG$_4$-MG$_6$ has three DERs, and MG$_7$ and MG$_8$ consist of five and ten DERs, respectively. All DERs are droop-based. It is obvious that the number of substitutions are larger than the number of determining inputs in each case. Moreover, one can consider approximate average calculation times for determining inputs as a fast manual process and substituting equations as a slow manual process fairly as 30 s and 4 min, respectively. Therefore, the total calculation time of substitution method for same case studies is much more than the corresponding time of the interconnection method. In addition, substituting equations may lead to different nested forms, which causes long calculation times or even manual calculation errors. Nonetheless, determining inputs is a straightforward MATLAB coding without arithmetic complications.

2.3. Simplified modeling methods

Fig. 10 shows a classification of both existing simplification methods used in IMG modeling and potential methods to improve it. Solid black boxes show all simplification methods studied in the IMG literature. Dashed red boxes indicate methods not studied or less studied in the IMG literature and gray boxes are used for correlated explanations and illustrations.

The simplified modeling methods can be organized into three clusters, i.e. MOB, MDB, and MEB simplification techniques. In the first cluster, the detailed model should be obtained at first, which is a disadvantage, then its order can be reduced using aggregation and perturbation methods [156]. The perturbation methods including regular (e.g., [157]) and singular types have often been used in the MG [130–134] and IMG [68,152] dynamic studies. In [70], dominant dynamic modes of CB-IMGs with a similar behavior are aggregated to one dynamic mode using an aggregation-based MOB method.

MDB methods try to find the simplified model without calculating a detailed model. The dominant modules in the desired dynamics are preserved and the others are removed according to the knowledge of the system, e.g. [51,62] (see Table 1). In [51], each DER within

IMGs is simplified just by the droop characteristics and other modules are deleted. Similar deletion method is used in [65,67] while DERs are considered of PQ-controlled type and their control is simplified to measurement LPFs and PI controllers. In [62], the Kron reduction method is used to simplify the IMG power network and the module aggregation method is used to aggregate similar modules, e.g. droop-based control units or transformers. Although Thevenin's theorem has been used in dynamic modeling of islanded MGs [158,159], it is still not used in IMGs.

MEB Methods benefit from the measured data and system identification techniques to find the model with a minimum computational burden, e.g. fast Fourier transform and Prony analysis to focus on the desired variable e.g. frequency. Despite being appropriate for large-scale systems, MEB methods are rarely used in IMG modeling [153] and model validation [90]. Nevertheless, Prony analysis has been used for another application, i.e. verification of small-signal models of CB-IMGs [38] and BTBC-IMGs [86,90] by comparing them with equivalent nonlinear real-time models.

According to dominant/non-dominant dynamic modes in the desired dynamics, a simplified model can be obtained by dividing all system variables into preserved and removed state variables. The model (6) shows both group state variables and their interactions, which can be decoupled using one of the simplification methods.

$$\dot{x}_{IMG}^{pp} = A_{IMG}^{pp} x_{IMG}^{pp} + A_{IMG}^{pr} x_{IMG}^{pr}, \tag{6a}$$

$$\dot{x}_{IMG}^{rr} = A_{IMG}^{rp} x_{IMG}^{rp} + A_{IMG}^{rr} x_{IMG}^{rr}. \tag{6b}$$

where superscripts "p" and "r" represent the preserved and removed states. The preserved states compose a reduced-order model. Note that (6) is a closed-loop model obtained from (4).

2.4. Comparison study: Oscillatory dominant modes of detailed and simplified models

Modeling of IMGs, particularly CB-IMGs, is intensively related to individual MG modeling methods. Here, an individual MG with a common structure of two droop-based DERs is considered to compare the most significant MG dynamic features, i.e. the dominant modes for detailed and simplified MG models. The data package [151] provides a MATLAB m-file, which can be useful for dynamic modeling similar to the case studied here. A sensitivity analysis for $\omega - P$ droop gain as $0.001 < k_1^P(P_{max1}/\omega_n) < 0.02$ is provided in Fig. 11 to compare the models, which are usually named by the model order of DER inverter and the simplification type, i.e. MDB or MOB. The simplified models consist of an MDB 5th-order model [70], an MOB 5th-order model [130], an MOB 4th-order model [134], and an MOB 3rd-order model [133]. The preserved state variables for such models are shown in Table 3. Furthermore, the detailed model [127] is considered as the reference model, where its order is 28. The oscillatory dominant modes, caused dominantly by the droop controllers, are of interest and non-dominant modes are not shown. Please note that these oscillatory modes are also exist in all types of ac IMG models, but other participants except the droop controllers like the inter-MG secondary controllers have a considerable participation factors.

By increasing DER$_1$ $\omega - P$ droop gain k_1^P, all the reduced-order models have a lower tendency to instability with respect to the detailed
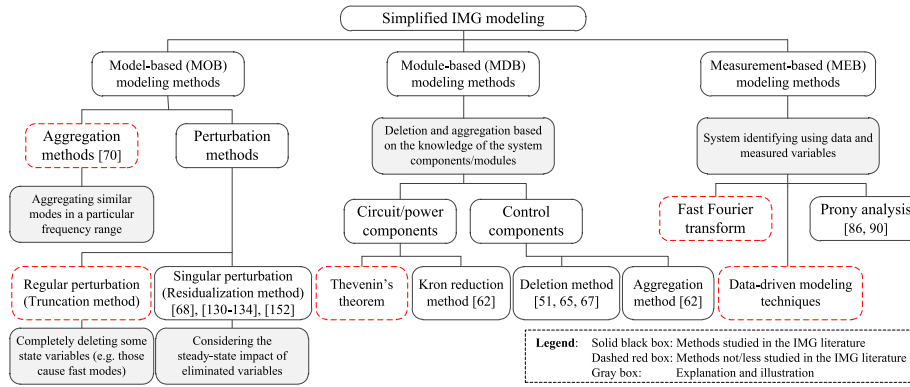
Fig. 10. Classification of simplified modeling methods including both studied cases in IMG modeling and those having considerably potential to be used.
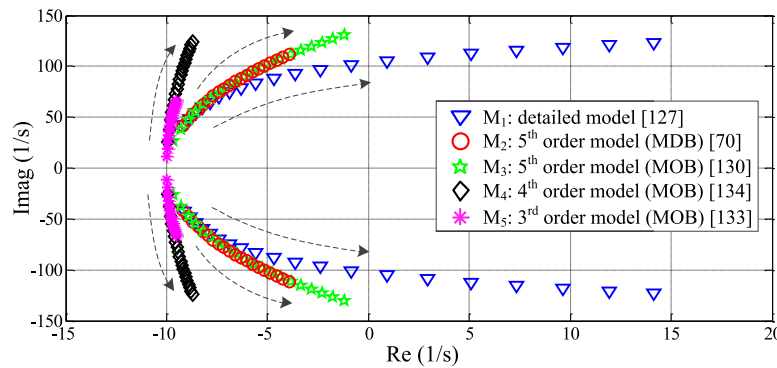

Fig. 11. Sensitivity analysis of oscillatory dominant modes of detailed and simplified models for $0.001 < k_1^P(P_{max1}/\omega_n) < 0.02$, (MDB: module-based simplified model, MOB: model-based simplified model).

Table 3
State variables of the compared models in Fig. 11.

Model	State variables	Ref.
M1	$\Delta\delta, \Delta P, \Delta Q, \Delta v_{odq}, \Delta i_{ldq}, \Delta i_{odq}$, CCIO[a], VCIO[b]	[127]
M2	Droop-based DGU: $\Delta\delta, \Delta P, \Delta Q, \Delta i_{odq}$ PQ-controlled DGU: $\Delta\delta_{PLL}$, CCIO, PLLIO[c]	[70]
M3	$\Delta\delta, \Delta P, \Delta Q, \Delta i_{odq}$	[130]
M4	$\Delta\delta, \Delta P, \Delta i_{odq}$	[134]
M5	$\Delta\delta, \Delta\omega, \Delta V_{od}$	[133]

[a] Current controller integrator outputs.

[b] Voltage controller integrator outputs.

[c] Phase-locked loop (PLL) integrator output.

model. Order reduction leads to a decrease of the model accuracy. Therefore, 5th-order models [70,130] are more accurate. Note that there exist medium-order simplified models [57,62,73], which are much more accurate than the 5th-order models in terms of dynamics and transients. Nevertheless, modeling simplicity of the low-order MDB model [70] is more than the MOB model [130], which is discussed in [70].

3. Stability analysis of interconnected microgrids

Fig. 12 shows the stability classification of islanded/interconnected MGs. Regarding MG/IMG components location, the stability can be divided into control system stability and power supply/balance stability. According to the controlled device type, the first can be classified into electric machine stability and power-electronics converter stability. According to control infrastructure, stability of physical parts, e.g. inner loops is addressed as communication-free stability and stability of cyber

environments is called communication-related stability. On the other hand, the second is classified into voltage and frequency stabilities. The MG voltage is stable if both dc link voltage of converters and ac voltage are stabilized using distributed local controllers. Frequency stability is two-fold including intra-MG and inter-MG balance stabilities. Moreover, stability is generally small-signal or large-signal in terms of disturbance size and is short-term or long-term in terms of disturbance duration. The main classification in Fig. 12 is from [160] and the complementary classification, indicated in red blocks, are added here.

According to Table 4, the IMG stability fields of research are classified based on IMG structure, stability analysis type and method, and study group. Furthermore, the special case studies and most important features are determined. Both small-signal and large-signal stability analyses are taken into account to investigate the stability challenges of different IMG structures, especially CB-IMG and BTBC-IMG, which are paid attention to the following subsections.

Several stability analysis methods are used in the IMG literature and mentioned in Table 4. Eigenvalue analysis (EA) is the fundamental tool of small-signal stability analysis, which can only determine stability/instability for a specific operating point. Participation factor/matrix (PF) adds the ability of determining the amount of being influenced for each eigenvalue and by each state variable, i.e. the corresponding module. Sensitivity analysis (SA) extends PF for a range of parameter values or operating points and results in loci of eigenvalues, which can visualize the impact of parameters or initial condition variations. TDSs, real-time simulations (RTSs) and experimental results (ERs) are powerful methods to analyze large-signal stability using nonlinear models and real laboratory setups. Though the ERs have more accuracy, the TDS and RTS are more suitable for stability studies due to the possibility of instability. Lyapunov theorem (LT) is another tool with a powerful mathematical basis to assess large-signal stability. Nevertheless, it is practically limited to low-order models. Other IMG stability
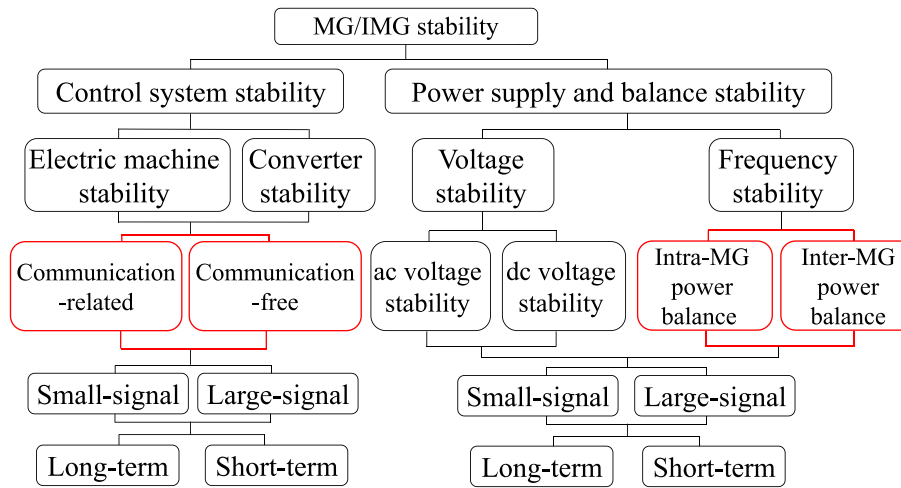
Fig. 12. Stability classification for islanded/interconnected microgrids.

analysis techniques include frequency response (FR), critical clearing time (CCT), kernel reflection (KR), phase portrait (PP), formal analysis (FA), Gershgorin theorem (GT) and methods based on measured data (MD).

3.1. Small-signal stability analysis

This stability type is analyzed based on the linear/linearized model around an operating point. For the model represented by the state-space theorem, e.g. (4), (5), or (6), the small-signal stability can be assessed using eigenvalue analysis as:

$$|\lambda I - A_{IMG}| = 0, \tag{7}$$

where λ shows the eigenvalues and I is the identity matrix. To have an asymptotic stability, all eigenvalues should have negative real values.

3.1.1. CB-IMGs

One can say the most challenging stability issue of a group of autonomous MGs interlinked through CBs is frequency stability and oscillations due to their direct power interactions. Compared to BT-BCs, CBs have no individual control units to regulate the IL power. Therefore, inter-MG power imbalances and instability are probable, if an IL power controller is not employed in high MG control levels, e.g. secondary controller [64,70,94]. It is also designed in the second layer of a two-layer four-level IMG power sharing control [57,73]. For such controllers, the stability is analyzed, and the stabilizing gain ranges are attained. From the IMG power side viewpoint, various physical interconnection points are compared via small-signal stability tools to form more stable MG clusters [68]. On the other hand, eigenvalue, participation factor and sensitivity analyses demonstrate the considerable impact of $\omega - P$ droop control on the IMG stability margins [64,68,95,96]. Other researches on the CB-IMG small-signal stability deal with delay-dependent stability [37] and formal analysis in the presence of heterogeneous uncertainties [65,67].

3.1.2. BTBC-IMGs

The synchrony is not important and challenging in BTBC-IMGs due to the existence of BTBC dc-link among MGs. Therefore, MGs with different rated frequencies/voltages are able to be interconnected. Although there are not the inter-MG modes due to frequency/voltage interaction, some critical modes appear due to dc-link voltage control and its interaction with MG controllers [87,158]. In fact, the dc-link voltage controller is the main reason for instability. Furthermore, the frequency/voltage instability in an MG is still able to be transferred to other linked MGs via the dc-link voltage. A virtual friction control

is represented in [161] to damp oscillations in conventional multi-area power grids connected via high voltage dc link, which can also be useful to apply to BTBC-IMGs, with modern generations.

3.1.3. DC-IMGs

The instability and oscillations are also addressed in DC-IMGs on dc bus voltages due to time delays of communication channels used in distributed controllers [113,116]. The IL controllers and their communication weights have a remarkable effect on the IMG stability as they form the highest level of control hierarchy, which by changing their gains easily move the dominant low-frequency modes [116,117]. Moreover, increasing controller gains, particularly secondary and tertiary control gains, decreasing IL length and inner MG lines length cause also reduction in the stability margins or even lead to instability [116]. In [110], the open-loop stability of the dc–dc converter used as interlinking device and power exchanger is analyzed, which shows the stability margin decreases by increasing the duty cycle.

3.1.4. Dominant eigenvalues of CB and BTBC IMGs

A CB-IMG including three MGs interconnected via three lines and three CBs, and a BTBC-IMG including three MGs interconnected via three lines and three BTBCs are considered, where the complementary information is accessed in [70,87], respectively. Moreover, the data package [151] includes some files, which are useful for linear and nonlinear modeling as well as small-signal and transient stability analysis of IMGs. The dominant eigenvalues as the most significant contributors in IMG small-signal stability are shown in Fig. 13. A simplified model of the CB-IMGs, including three dynamic modes for each MG, is considered to obviously see the MGs interactions. On the other hand, the detailed model of the BTBC-IMGs is used to recognize the most effective IMG parts on stability.

Inter-MG interactions are the main cause of the frequency instability and the oscillations in CB-IMGs. According to Fig. 13(a), $\lambda_1 - \lambda_6$ are the main inter-MG modes affected by all IMG modules including MG power components, primary controllers, secondary controllers, and the IL power exchanges. $\lambda_{7,8}$ are the non-oscillatory modes affected only by the secondary controllers. The main interactions are of oscillatory type, which can lead to frequency oscillations and instability, particularly for low-inertia power electronics-based IMGs.

As shown in Fig. 13(b), critical dominant modes in the BTBC-IMGs are due to interactions of $\omega - P$ droop controllers and PLLs as well as interactions of power dc side and dc voltage controller of BTBCs. The first are oscillatory types, however the second are also critical. To achieve more reliable stability analysis results, different operation points should be considered, e.g. using sensitivity analysis [57,73,87].

Table 4

Literature review of stability analysis of interconnected microgrids.

Reference	IMG structure	Stability type	Stability analysis method							Study group	Case study/Important feature
			EA	PF	SA	TDS	ER	LT	Other		
[12]	Hybrid ac/dc	Small-signal	✓		✓	✓				Component influence	Static/dynamic load stability
[13]	Hybrid ac/dc	Small-signal				✓			FR	Phenomena stability	Mitigating low-frequency oscillations
[35]	Two ac IMG	Large-signal				✓			CCT	Stability improvement	Inertia emulation by Synchronverter to increase IL power capacity
[113]	dc IMG	Small-signal	✓			✓			KR	Phenomena stability	Time-delay stability of distributed control and related oscillation proof
[137]	CB-MIMG	Large-signal				✓				Stability improvement	Robust MG clustering in dist. grids
[61]	CB-MIMG	Small-signal				✓			PP	Phenomena stability	Determining maximum penetration level of MGs to the main grid
[94]	SS-MIMG	Both	✓	✓	✓	✓				Controller stability	power exchange controller stability
[117]	dc IMG	Both	✓		✓			✓	FR,RTS	Controller stability	Stabilizing power exchange controller
[37]	CB-MIMG	Both	✓			✓		✓		Phenomena stability	Enhancing delay-dependent stability by disturbance attenuation stabilizer
[57,73]	CB-MIMG	Small-signal	✓	✓	✓	✓				Stability improvement	Analyzing control parameters and low-damping oscillation
[72]	CB-MIMG	Large-signal				✓		✓		Controller stability	Controller asymptotic stability proof
[14]	Hybrid ac/dc	Small-signal	✓		✓	✓				Component influence	Establishing stability margins of ILDs
[65,67]	CB-MIMG	Small-signal							FA, GT	Components influences	Stability assessment by reachable set
[85]	BTBC-MIMG	Small-signal	✓		✓	✓				Controller stability	Designed controller stability analysis
[116]	dc IMG	Both	✓	✓	✓	✓	✓			Controller stability	Designed controller stability analysis
[68]	CB-MIMG	Small-signal	✓		✓	✓				Stability improvement	Critical clusters stability assessment
[63]	CB-MIMG	Large-signal				✓				Component influence	Resilient self-healing operation using multi-agent system coordination
[118]	dc IMG	Large-signal				✓		✓		Controller stability	Designed controller stability analysis
[95,96]	CB-MIMG	Small-signal	✓	✓	✓	✓				Component influence	Wide stability analysis of parameters
[66]	CB-MIMG	Large-signal							MD	Stability improvement	Improving dynamic stability/resilience
[27]	CB-MIMG	Large-signal				✓			CCT	Component influence	Transient stability assessment
[110]	dc IMG	Both	✓					✓	RTS	Controller stability	Designed controller stability analysis
[51,59,69]	CB-MIMG	Both	✓			✓		✓		Component influence	Different stability/security assessments
[64]	CB-MIMG	Small-signal	✓	✓		✓				Component influence	Stability analysis of PV-based IMGs
[87,89]	BTBC-MIMG	Both	✓	✓					RTS	Component influence	BTBC parameter impact on stability
[70]	CB-MIMG	Small-signal	✓	✓		✓				Phenomena stability	Introducing inter-MG dynamic modes
[105]	Multiple ac–dc	Small-signal	✓		✓				FR	Component influence	Introducing inter-MG dynamic modes

EA: eigenvalue analysis, ER: experimental results, FR: frequency response, LT: Lyapunov theorem, PF: participation factor, SA: sensitivity analysis, TDS: time-domain sim., CCT: critical clearing time, KR: kernel reflection, PP: phase portrait, FA: formal analysis, GT: Gershgorin theorem, MD: measured data, RTS: real-time sim.

3.2. Large-signal stability analysis

Although the operating point is fixed in small-signal stability and small changes around it is acceptable, it can change in a large range for large-signal/ transient stability assessment. Power systems Large-signal stability can be assessed by graphical, direct, time-domain, and automatic learning methods [162]. The graphical methods consist of equal-area criterion and phase portrait, which are mostly used in conventional one-machine power systems [163]. The direct method employs Lyapunov functions, which are more applicable for low/reduced-order systems [37,51,59,69,72,118]. The automatic learning methods benefit from intelligent algorithms such as artificial neural networks to assess transient stability [164]. Usual time-domain assessment criteria are the critical clearing time (CCT) and the power transfer limit (PTL) [35, 165,166]. However, operating point changing is common to study for the stability and system behavior without using the aforementioned criteria.

3.2.1. CB-IMGs

Lyapunov theorem (LT) is mostly used to guarantee asymptotic stability [37,51,59,69,72]. However, linear IMG models are used and thus the stability proof cannot be considered as a transient stability proof. In [37], time delays and uncertainties are included in the Lyapunov

function. Using TDS as another common tool for large-signal stability assessment, LT-based transient stability proof is validated [59,72]. In another application, weaker synchronism of two IMGs with respect to an individual MG is shown using CCT. The transient stability of CB-IMG is also taken into account in terms of resilience [63,66], and clustering robustness [137].

3.2.2. BTBC-IMGs

In [87], the dc voltage of BTBCs among IMGs is focusing on transients, especially at initial instants of power exchange. Therefore, a minimum stabilizing initial dc voltage value is proposed as a transient stability margin of BTBC-IMGs.

3.2.3. DC-IMGs

Multiple operating points are considered and large-signal stability is assessed using TDS [110,118], real-time simulations (RTSs) [110, 116,117], and experimental results [110,116] for synthesized IL power controllers. Various scenarios including modifying power reference and bus voltages [110], fault condition and communication delay on the IL controller [116], instability test of violating control gains, MG plug-and-play capability, CPL capacity increase, and communication delay [117], and global/local layer link failure and time delay [118]
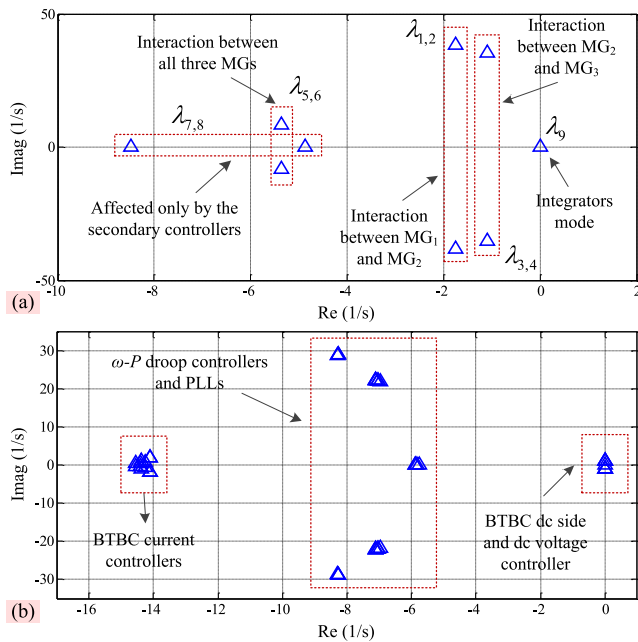
Fig. 13. Dominant eigenvalues of (a) simplified model of the CB-IMGs and (b) detailed model of the BTBC-IMGs.

Fig. 14. Frequency oscillations and their propagation in CB-IMGs and BTBC IMGs: (a) frequency changes of MG_1 and MG_2 in three CB-IMGs, (b) frequency changes of MG_1 and MG_2 in three BTBC-IMGs, (c) dc link voltage of BTBC in three BTBC-IMGs.

are taken into account to validate the corresponding controllers performance and transient stability. Moreover, an LT-oriented asymptotic stability proof is represented in [117,118].

3.2.4. Frequency oscillation/instability and its propagation

Here, frequency oscillations, the possible corresponding instability, and their propagation through ILDs is studied. Fig. 14 shows the outputs of two case studies. The first one is a CB-IMG with three MGs, where the details of the system can be found in [70]. The MG_1 load is increased as 50% of the overall IMG rating at $t = 1$ s as a large-signal disturbance. Fig. 14(a) shows the frequency changes of MG_1 and MG_2 after the load increases. Frequency oscillations appear in MG_1 and are immediately spread to MG_2 through the ILD, i.e. a CB. The frequency oscillations propagate with a very low delay due to IL dynamics.

The second case is a BTBC-IMG with three MGs. More details of the studied system is addressed in [87]. Fig. 14(b) similarly shows the frequency changes of MG_1 and MG_2, while IMGs are islanded before $t = 0.5$ s. They are connected hereafter while PLL integral gain of the BTBCs equals 0.5 as a dominant parameter in IMG stability. The gain increases to 2.6 at $t = 2$ s for the PLL of BTBC MG_2's side, which is as large as cause instability. The frequency changes in MG_2 are very large and the frequency destabilizes so fast. However, the MG_1 frequency instability is much slower and the oscillation amplitude is very small. The BTBC among these two MGs propagates the frequency oscillations through its dc link. Fig. 14(c) shows dc link voltage of the BTBC. Therefore, although the dc link can make an independent frequency control for BTBC-IMGs, oscillations and instability propagate through this link from an MG to another. Furthermore, dc voltage disturbances due to bad control and original dc link disturbances can deploy very fast via both ac voltages and frequencies, which are so harmful for weak IMGs and may easily cause instability [35,87].

4. Control of interconnected microgrids

The IMG control can be studied from different viewpoints. According to the control architecture, it can be classified into centralized, decentralized, and distributed. All the three architectures can be realized in a standard hierarchical form including three [138]/four [1]
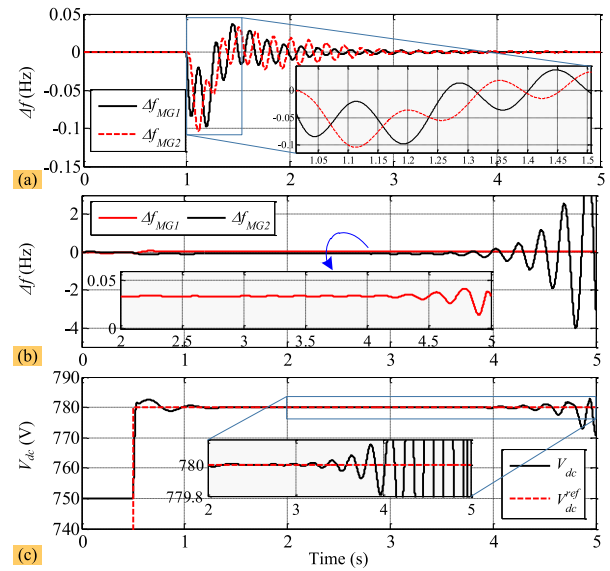
control levels, i.e. primary, secondary, central-emergency, and tertiary/global layers. Concepts and literatures of these architectures and control layers for islanded MGs are reviewed in [149]. In IMGs, there exists a vital control objective added with respect to islanded MGs, which is power exchange/sharing control among IMGs. It is the main control objective specific to IMGs that requires satisfying some secondary or higher level objectives like cooperated frequency control in CB-IMGs and power and dc voltage control aims of BTBCs in BTBC-IMGs. These special IMG control objectives can be considered in the existing control layers of the MG hierarchical control structure. The point that the IMG power exchange controller is realized in which control layer, i.e. primary, secondary or tertiary, leads to another classification of the IMG control. For instance, main control layers specific to IMGs are fully implemented in the primary layer [26,48], the secondary layer [23,94], and the tertiary layer [75,80]. However, it is realized in some literature via two control layers, e.g. primary and tertiary layers [37] or secondary and tertiary layers [114].

Table 5 reviews the IMG control literature with the useful classifications from several aspects, validation methods and main control objectives. The IMG structure and control architecture investigated in the literature, and the control layer i.e. primary control (PC), secondary control (SC), and tertiary control (TC), selected to implement the special IMG control objectives, are mentioned in the second, third, and fourth columns, respectively. In the fourth column, hierarchical control (HC) means that the IMG control aims are distributed in all three layers, and BTBC and dc–dc converter (DDC) indicate that a part of IMG controllers are realized at their controllers. A relative level of Communication channel bandwidth used for IMG control is addressed in the fifth column. Furthermore, control type/design methods and controller validation techniques are presented in the sixth and seventh columns, and the corresponding illustrations for the abbreviations can be found at the bottom of Table 5. The final column consists of main and ancillary control objectives of different IMG structures investigated in the literature.

IMG control can be divided into two categories in terms of the need to communicate data. Different topologies of the decentralized control architecture [29,84], which are usually used for emergency power exchange and critical MG restoration, are generally free from communicating data. Nonetheless, centralized [91] and distributed [57] control

Table 5
Control literature review of interconnected microgrids.

Reference	IMG structure	Control architecture	Control layer	Telecom bandwidth	Control type/ Design method	Validation method	Main control objective
[26]	Two IMG	Decentralized	PC	None	PR	TDS, ER	Coupling effects among MGs
[28,34,91]	BTBC-MIMG	Centralized	BTBC-TC	High	PI	FR, TDS	Basic power sharing ideas
[99]	ac/dc MIMG	Centralized	HC	High	PI, AD	TDS	Economic operation of on/off-grid IMGs
[20,21,23]	Two IMG	–	SC	–	LFC, FL	LMTDS	Theory of IMG load-frequency control
[25]	CB-MIMG	Distributed	HC	Very low	PI, CP, MAS	TDS	Network topology-based power exchange
[94]	SS-MIMG	Distributed	SC	Low	PI, CP	TDS, ER	Voltage and power exchange control
[114]	dc IMG	Distributed	SC, TC	Low	PI, VI, MAS	RTS	Coordinated power flow control
[37]	CB-MIMG	Centralized	PC, TC	High	Robust droop	TDS	Adaptive power flow control
[57,73]	CB-MIMG	Distributed	HC	Low	I, CP, PSO	TDS	Four-level power sharing
[93]	BTBC-MIMG	Distributed	BTBC-TC	Low	Robust	TDS	Transient stability improvement
[92]	BTBC-MIMG	Centralized	TC	High	PI, AD	TDS	Power exchange via dc lines
[120]	dc IMG	Centralized	DAB-PC, TC	High	IOL	TDS	Coordinated control of energy storages
[33,84]	BTBC-MIMG	Decentralized	BTBC-TC	None	PI	TDS	Frequency control improvement
[29–31]	Two IMG	Decentralized	BTBC-PC	None	PI, droop	ER	Active/reactive power exchange
[88]	BTBC-MIMG	Decentralized	BTBC-PC	None	PI, droop, LC	RTS	Emergency frequency/voltage support
[108,109]	dc IMG	Decentralized	DDC-PC	None	PI	TDS	Interconnection of dc IMGs
[72,79]	CB-MIMG	Distributed	SC	Low	I, PC	TDS	Cooperative IMG power sharing
[115]	dc IMG	Distributed	HC	Low	PI, FTCP	TDS	Power management enhancement
[44,70]	CB-MIMG	–	SC	–	VI	LMTDS	Frequency control improvement
[75]	CB-MIMG	Distributed	TC	Very low	PI, CP, ET	TDS	Event-triggered Power sharing
[80]	CB-MIMG	Distributed	TC	Low	MAS	TDS	Fully distributed IMG control
[46]	CB-MIMG	Distributed	SC	Low	I, PCP, MAS	TDS	Grid-feeding/forming DER role in IMG
[116]	dc IMG	Distributed	HC	Low	PI, PCP	RTS, ER	Economic tie-line power control
[36]	Two IMG	Centralized	PC, TC	Low	AD, LC	TDS	Fast IMG forming during power shortfall
[45]	CB-MIMG	Distributed	SC	Very low	I, CP, ET	RTS, ER	Software-defined power sharing
[118]	dc IMG	Distributed	SC	Low	PI, PCP	TDS	Improving dynamic performance of IMGs
[48]	CB-MIMG	Decentralized	PC	None	PI	TDS	Improving frequency response
[112]	dc IMG	Distributed	SC	Low	PI, CP	RTS	Power exchange based on battery storages
[110]	Two dc IMG	Decentralized	DDC-PC	None	PI	RTS, ER	Active power flow control
[100]	ac/dc MIMG	Distributed	SC	Very low	PI	TDS, ER	Asynchronous power control
[111,121,122]	dc IMG	Distributed	–	Low	PI, HSS	TDS	IMG power flow control
[76]	CB-MIMG	Distributed	SC	Very low	I, PCP, ET	TDS	Reducing communication burden
[71]	CB-MIMG	Decentralized	PC	None	PI, VI	TDS	Virtual inertia to improve stability
[83]	BTBC-MIMG	Decentralized	PC, SC	None	AD, LC	TDS	IMG control in various operating points
[98]	ac/dc MIMG	Distributed	TC	Very low	PI, CP, ET	TDS	Power support by a low communication
[101]	ac/dc MIMG	Centralized	HC	High	PI, PR	TDS, ER	Energy pool for power exchange

PC: primary control, SC: secondary control, TC: tertiary control, HC: hierarchical control, PI: proportional–integral, PR: proportional-resonance, AD:adaptive droop, FL:Fuzzy logic, CP: consensus protocol, FTCP: finite-time CP, VI: virtual inertia, LMTDS: linear model TDS, IOL: input–output linearization,DDC: dc–dc converter, ET: event-triggered, MAS: multi-agent systems, HSS: Hamiltonian surface shaping, LC: logic control, I: integral, DAB: dual active bridge.

architectures require a level of communication data. In general, distributed control methods are a solution to reduce data communication of centralized approaches and solve correlated challenges using consensus protocol [115], multi-agent systems [114] etc. Moreover, distributed control techniques are improved to more reduce communication burden, e.g. using an event-triggered communication method [75, 76] or a Q-learning algorithm [25].

Various controller types and design methods, e.g. proportional–integral (PI), proportional-resonance (PR), modified droop, and robust designs are used in IMG controllers to improve achievement of IMG control goals. The most common controllers are PI, droop, and integral (I) for inner, primary, and secondary control layers, respectively due to their simplicity. Adaptive droop (AD), generalized and robust droops, and virtual inertia (VI) are enhancements of the simple droop method in the primary control level. In addition to improving the inertial response of each MG [167], VI methods can increase the damping of IMG power

exchanges [71], enhance the transient stability of weak IMGs [35], and improve the load-frequency control (LFC) [44]. Consensus protocol (CP), finite-time CP, which can be converged within a finite time, multi-agent systems (MAS) usually used for coordinated control of complex systems, e.g. IMGs, and, event-triggered (ET) algorithms for reducing communication burden, are the common communication infrastructures investigated in IMGs.

4.1. Control of CB-IMGs

Decentralized control cases are limitedly represented [48,71]. In [48], a simple MG structure including one grid-forming DER and a number of grid-feeding DERs is considered, where the need of coordinated control is eliminated to focus on the primary frequency dynamics. A modified automatic voltage regulator is proposed for the grid-forming DERs to improve the frequency response. The same objective is taken
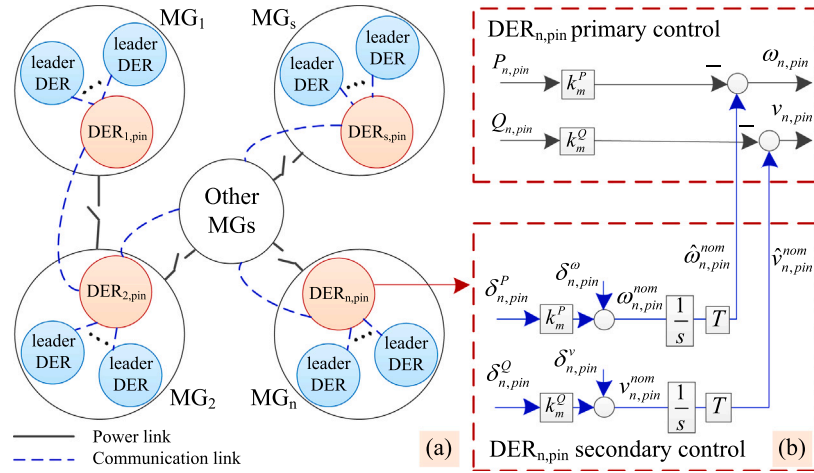
Fig. 15. Control of CB-MIMG: (a) pinning consensus-based distributed secondary control architecture, (b) corresponding uniform control structure, where the input signals are existing in Table 6 [72,76].

into account by virtual inertia control using super-capacitors without considering the control architecture [71]. Therefore, one can say CB-MIMG control just at the primary level without data communication is impossible.

In [37], a wide-area measurement and communication system including MG central controllers and a global distribution system control is represented. Nevertheless, most of the CB-MIMG literature belongs to distributed control methods, which seem to be the most reasonable solution to control power exchange among such IMGs.

The distributed IMG control is realized in secondary and tertiary levels or by a complete hierarchical control (see Table 5). Some authors have tried to find a standard method like the tie-line power control of traditional power systems. Hence, the IMG control is implemented in the secondary control level with the aims of IMG active/reactive power sharing and global frequency/voltage regulation. Generally, the pinning consensus protocol is used in which one of the DERs in each MG is selected as a leader (pinning) agent. Fig. 15(a) shows the communication type in the pinning consensus-based distributed secondary control architecture for CB-MIMGs. Therefore, in a two-layer communication infrastructure, DER_{pin} is as a leader for follower DERs within the MG to determine the nominal voltage/frequency in the intra-MG layer, and it is a communicating node in the inter-MG layer to share the information with the other MG leaders.

Fig. 15(b) shows a uniform control structure for the leader DER in MG_n. The error signals $\delta_{n,pin}^{\omega}$, $\delta_{n,pin}^{v}$, $\delta_{n,pin}^{P}$, $\delta_{n,pin}^{Q}$, which are the inputs of the integral secondary controller, are listed in Table 6. In [57,73], the same method is utilized, however the MG PCC data is the basis of the inter-MG layer communication instead of the pinning DERs data, which leads to the excess measurement and thus a lower reliability.

4.2. Control of BTBC-IMGs

Fig. 16 shows the control architectures of BTBC-IMGs. A decentralized control for BTBC-IMGs is realized using droop characteristics. Modified droop characteristics are used in controlling interlinking VSCs to consider MG overload and over-generation conditions [29,31,83,84], e.g. (8) of [83] using the SOC and nominal power P_n of energy storage systems as droop-based DERs.

$$\omega = \begin{cases} \omega_n - k_p(P - P_n), & \begin{aligned} & P \leqslant P_n \& SOC \geqslant SOC_{\max} \\ & P > P_n \& SOC \leqslant SOC_{\min} \end{aligned} \\ \omega_n, & \begin{aligned} & P > P_n \& SOC < SOC_{\max} \\ & P \leqslant P_n \& SOC > SOC_{\min} \end{aligned} \end{cases} \quad (8)$$

A generalized droop is also used to determine active and reactive power references in (13) and (19) of [88]. In such a decentralized control

architecture, as shown in Fig. 16(a) frequency and/or voltage are locally being measured to detect the emergency condition by applying logic functions [33,83,88]. Furthermore, the control signals u_f and u_v are provided for the BTBC by applying generalized/modified droop characteristics, i.e. F_f and F_v, on the frequency and voltage differences in order to exchange enough active and reactive powers between the MGs. In this architecture, generally, there is no communication and power exchange with other MGs.

By communicating some useful information, e.g. DERs surplus powers, centralized control architecture is employed in order to increase the control precision [28,92]. Fig. 16(b) shows a centralized control architecture for BTBC-IMGs, where the IMG central controller has a wide communication with tertiary/central control of MGs and BTBC controllers. It requires the current status of both MGs and BTBCs. For example, it requests and receives maximum allowable power generation of MGs, i.e. p_{max}^{MG1}, p_{max}^{MG2}, ..., p_{max}^{MGn}, and the dc link voltage of BTBCs, i.e. $v_{dc,12}$, $v_{dc,1n}$, ..., $v_{dc,2n}$, to have a stable and optimal power exchange. Therefore, it determines a new power balance by sending the power references to MGs and BTBCs, e.g. p_{ref}^{MG1}, $p_{ref}^{1,n}$ and p_{ref}^{MGn} for a power exchange between the MG_1 and the MG_n through the $BTBC_{1n}$. Although such a coordination among MGs and BTBCs is necessary, communicated information and required paths can be represented in a different form to improve the communication system performance.

The communication is minimized and thus the reliability can be improved by replacing the distributed communication instead of the centralized one [93] as shown in Fig. 16(c). In the distributed architecture, there exists a distributed controller for each BTBC, which can communicate with that BTBC and adjacent MGs on one hand, and can communicate with neighbor distributed controllers on the other hand. All advantages of the distributed control architecture with respect to the centralized control architecture, which are discussed in [149] for the secondary control of autonomous MGs, can be considered here for BTBC-IMGs and generally IMGs by doing potential research. The details of communicated data are not shown in Fig. 16(c) due to its similarity to Fig. 16(b). However, more details can be found in [93].

Regarding the IMG operation, emergency or planned power exchange may occur. Though decentralized control is preferred in emergencies, centralized and distributed architectures are more applicable in planned operation, where MGs communicate their power shortfall/surplus to the controllers and accordingly the power set-points are determined and then sent to BTBCs [34,88,91,93]. (see Figs. 16(b) and 16(c)).

4.3. Control of DC-IMGs

The decentralized control architecture is implemented using dc–dc converters [108,109] and dual active bridge (DAB) converters [163]

Table 6

Pinning consensus-based distributed secondary control inputs for leader ders in CB-IMG correlated with Fig. 15.

Reference	Upper: $\delta_{n,pin}^{\omega}$, Lower: $\delta_{n,pin}^{v}$	Upper: $\delta_{n,pin}^{P}$, Lower: $\delta_{n,pin}^{Q}$
[45]	$\sum_{l=1}^{s} \tilde{a}_{nl}(\hat{\omega}_{l,pin}^{nom} - \hat{\omega}_{n,pin}^{nom})$	0
	0	0
[46]	$\sum_{l=1}^{s} \tilde{a}_{nl}\{(\omega_{l,pin} - \omega_{l}^{rated}) - (\omega_{n,pin} - \omega_{n}^{rated})\}$	$-\frac{1}{k_{n,pin}^{P}} d_{n,pin}(\omega_{n,pin} - \omega_{n}^{rated})$
	$\sum_{l=1}^{s} \tilde{a}_{nl}\{(v_{l,pin} - v_{l}^{rated}) - (v_{n,pin} - v_{n}^{rated})\}$	$-\frac{1}{k_{n,pin}^{Q}} d_{n,pin}(v_{n,pin} - v_{n}^{rated})$
[72]	$\sum_{l=1}^{s} \tilde{a}_{nl}(\omega_{l,pin} - \omega_{n,pin}) + \tilde{a}_{n0}(\omega^{rated} - \omega_{n,pin})$	$\frac{1}{k_{n,pin}^{P}} \sum_{l=1}^{s} \tilde{a}_{nl}(k_{l,pin}^{P} P_{l,pin} - k_{n,pin}^{P} P_{n,pin})$
	$\sum_{l=1}^{s} \tilde{a}_{nl}(v_{l,pin} - v_{n,pin}) + \tilde{a}_{n0}(v^{rated} - v_{n,pin})$	$\frac{1}{k_{n,pin}^{Q}} \sum_{l=1}^{s} \tilde{a}_{nl}(k_{l,pin}^{Q} Q_{l,pin} - k_{n,pin}^{Q} Q_{n,pin})$
[76]	$\sum_{l=1}^{s} \tilde{a}_{nl}(\omega_{l,pin} - \omega_{n,pin}) + \tilde{a}_{n0}(\omega^{rated} - \omega_{n,pin})$	$\frac{1}{k_{n,pin}^{P}} \sum_{l=1}^{s} \tilde{a}_{nl}(k_{l,pin}^{P} P_{l,pin} - k_{n,pin}^{P} P_{n,pin})$
	0	0
[79]	$\sum_{l=1}^{s} \xi\tilde{a}_{nl}(\omega_{l,pin} - \omega_{n,pin}) + \tilde{a}_{n0}(\omega^{rated} - \omega_{n,pin})$	$sat(P_{n,pin}(0) + \frac{1}{T}\int_{0}^{t}\sum_{l=1}^{s} \xi\tilde{a}_{nl}(M_{l,pin}(s) - M_{n,pin}(s))ds)$
	$\sum_{l=1}^{s} \xi\tilde{a}_{nl}(v_{l,pin} - v_{n,pin}) + \tilde{a}_{n0}(v^{rated} - v_{n,pin})$	$-\int \omega_c Q_{n,pin} + \int \omega_c Q_{n,pin}^{measured}$

$\tilde{a}_{nl}$: nl'th array of the inter-MGs network adjacency matrix, $\tilde{a}_{n0}$: is 1 if the leader DER can receive the rated information, otherwise it is 0, $d_{n,pin}$: pinning control gain, M: leader DG increment cost, for $sat(.)$ and other variables see the references.
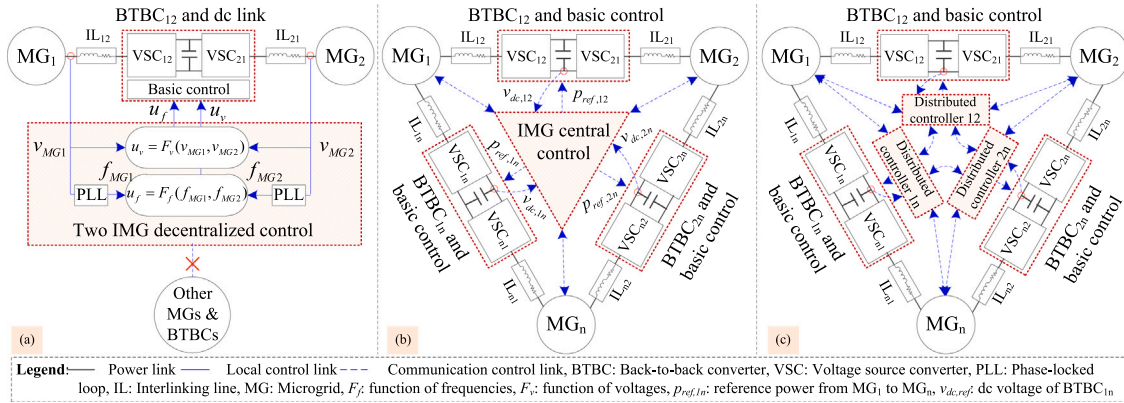

Fig. 16. Control Architectures of BTBC-IMG: (a) decentralized control [33,83,88], (b) centralized control [28,92], (c) distributed control [93].

as power exchange actuators. Similar to CB-IMGs, the most applicable control architecture is the distributed architecture (see Table 5). In [114], an averaging consensus method is used to communicate the PCC voltage and the average SOC of dc MGs, thus the voltage coordination among MGs and the power flow control are accomplished in the secondary and tertiary layers, respectively. A hierarchical control is employed to consider minimizing the power generation cost in the power exchange control [115,116]. A pinning consensus method is also used that approximately follows the general structure presented in Fig. 15 in which the $v - i$ droop is used. In order to feed the secondary controller, DER_{pin} voltage error [116,118], IL power error [116], and load current sharing error [118] are selected.

4.4. RTS: Active and reactive power support in BTBC-IMGs

Three MGs, interlinked through two BTBCs are considered. As shown in Fig. 16(a), each MG includes two DERs, and a decentralized control is used for BTBCs including both frequency and voltage signals to detect emergency and share power. However, a low bandwidth coordination control is used to coordinate emergency controllers of $BTBC_{12}$ and $BTBC_{13}$. The emergency detection thresholds of $BTBC_{12}$ are designed less than that of $BTBC_{13}$. The real-time simulation for such a system is done using an OPAL-RT digital simulator, where further information can be found in [88].

As shown in Fig. 17, MG_1 is overloaded at $t = 1$ s and it is quickly supported by MG_2 due to a lower detection threshold as well as enough

surplus power. MG_1 goes back to the normal condition at $t = 2$ s and MG_2 loses the spare power due to a local full load condition at $t = 3$ s. The similar MG_1 overload condition happens at $t = 4$ s, which is not supported by MG_2 and $BTBC_{12}$ emergency control due to the lack of MG_2 surplus power. Nevertheless, MG_3 and $BTBC_{13}$ compensate for the MG_1 overload with a larger delay due to a larger detection threshold. Finally, MG_1 goes back to the normal condition at $t = 6$ s, which is detected well and the MGs are forced to switch to the islanded operating mode.

4.5. TDS: Power sharing in CB-IMGs

In this scenario, three ac MGs are interconnected through two CBs and two lines in the general form of Fig. 15(a), where MG_1 and MG_2 are connected via CB_{12} and IL_{12} with $z_{IL12} = 1.6 + j0.6\ \Omega$, and MG_1 and MG_3 are connected via CB_{13} and IL_{13} with $z_{IL13} = 1.6 + j0.6\ \Omega$. Each MG consists of two DERs in which the pinning-based consensus distributed secondary controller [72] is used and DER_1 is selected as the leader DER. The rated power of DER_2 is twice that of DER_1. Helping files for simulations are represented in the data repository provided for IMG modeling and simulation [151].

Fig. 18 shows the simulation results for a sequence of events. The MGs are isolated till $t = 4$ s. The pre-synchronization starts from $t = 4$ s and a synchronization algorithm [168], is used, which causes satisfying synchronization thresholds, $\Delta f = 0.05$ Hz, $\Delta\varphi = 5°$, and $\Delta v = 5$ V, and finally closing CB_{13} at about $t = 5$ s. The synchronization control loops
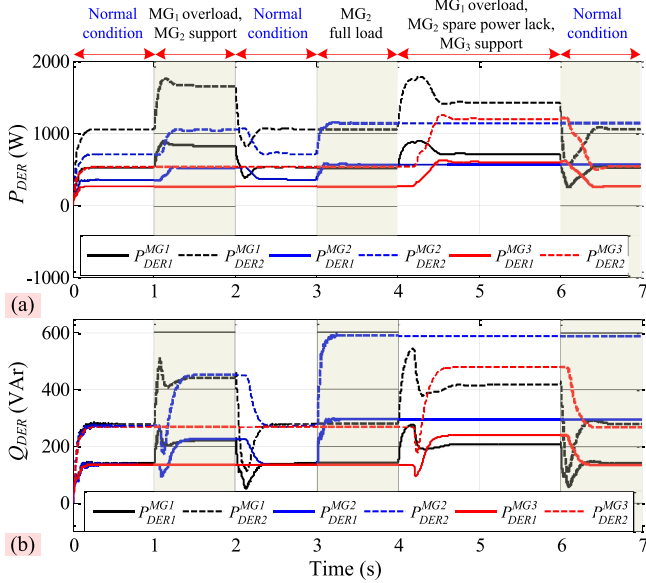
Fig. 17. MG$_1$ power shortage support by MG$_2$ in [1 2] s and MG$_3$ in [4 6] s under emergency detection and control for three BTBC-IMGs: (a) active power of DERs, (b) reactive power of DERs.

Fig. 18. Autonomous Operation, synchronization process, interconnection, and MG$_1$ load increase in three CB-IMGs: (a) pinning/leader DERs frequencies, (b) active powers of all DERs, and (c) exchanging active and reactive powers.

are opened at $t = 6$ s. IMG$_{13}$ including MG$_1$ and MG$_3$ goes to steady state in $t = (6, 8)$ s. Another interconnection is between MG$_1$ and MG$_2$, where pre-synchronization starts at $t = 8$ s, synchronization thresholds are satisfied and CB$_{12}$ is closed at about $t = 9$ s, and the synchronization control is off at $t = 10$ s. A load increase as 50% of the base load occurs in MG$_1$ at $t = 14$ s.

According to Fig. 18(a), frequency is controlled well during autonomous operation, synchronization transients, and the load change. As shown in Fig. 18(b), active power sharing is done in autonomous MGs before $t = 4$ s, in IMG$_{13}$ within $t = (6, 8)$ s, and in the complete IMG including the three MGs in $t = (12, 14)$ s. Furthermore, active power sharing is maintained for the MG$_1$ load increase. As shown in Fig. 18(c), power exchanges are zero before the IMG$_{13}$ formation at $t = 5$ s. In IMG$_{13}$, MG$_3$ sends the active power to MG$_1$ and the reactive power exchange is about zero during $t = (5, 8)$ s. In the complete IMG, MG$_2$ has the priority to support MG$_1$ with respect to MG$_3$ due to its lower own load. The MG$_1$ load increase is compensated by increasing local MG$_1$ generation shown in Fig. 18(b), as well as receiving power from both MG$_2$ and MG$_3$. The reactive power is also exchanged to improve bus voltages.

5. Research gaps

5.1. In dynamic modeling

In Fig. 10, the boxes with dashed red margin show the methods not used in IMG modeling despite their useful characteristics for simplifying such large-scale system models. The MOB aggregation method is very useful for clustering neighbor eigenvalues, which is less taken into account [70]. In MDB methods, Thevenin equivalent circuit, which is already used for multi-area power systems [169], can be used in case studies, where specific MG dynamics are of interest and other MGs and interlinking networks should be simplified.

Since IMGs are broad and complex systems, which lead to high-order models even using MOB and MDB modeling methods, MEB methods can be used to find very low-order models based on measuring just one specific variable, e.g. frequency. Fast Fourier Transform is a powerful tool to analyze measured data, which can be used in IMG frequency studies like those have been done for multi-area power
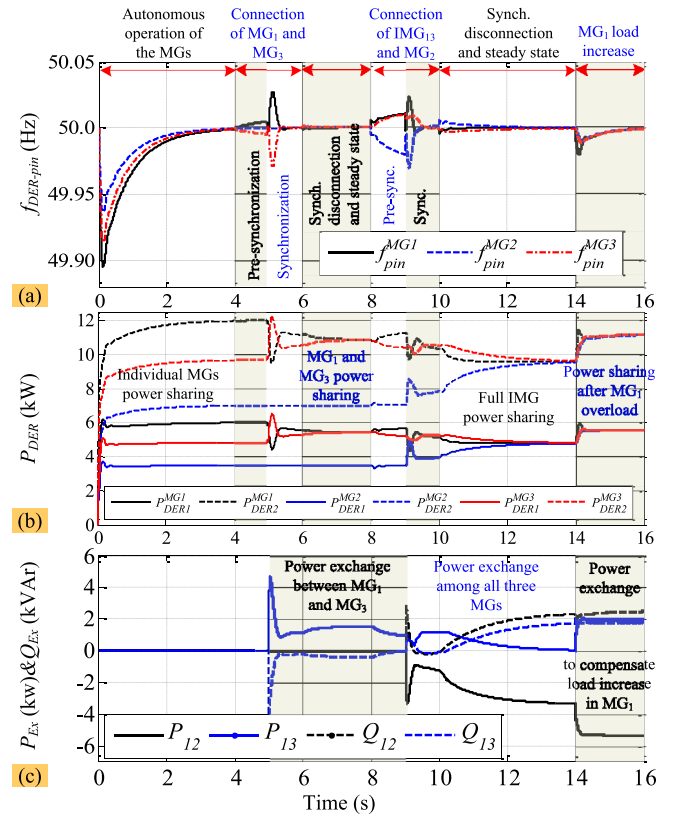
systems [170,171]. Other system identification and signal processing techniques including Prony analysis [172,173], discrete wavelet transform [170], and vector fitting technique [174] can be employed to analyze the measured data. Artificial-intelligence modeling techniques can be used [175,176] for both small-signal and large-signal modeling types. Electromagnetic transient and phasor-domain hybrid simulation methods can also be adapted from transmission and distribution dynamic co-simulation literature [177,178] to reduce the computational time of large-signal analysis.

Data-driven modeling techniques and machine learning methods will be very useful in new smart heavily data-oriented grids including IMGs. The modeling ideas can be adopted from the relevant literature, where data-driven methods and various machine learning algorithms are used for MG [179] and IMG [180] energy management, online detection of cyber attacks in peer-to-peer IMG energy trading [181], MG power management considering various climate conditions [182], and modeling DERs [183] and loads [184] in autonomous MGs.

On the other hand, many models on IMGs, reviewed in Table 1, are gained without an acceptable validation. In order to achieve standard IMG models to be used in different real and laboratory cases, secure and validated models are required. Data-driven approaches and other MEB methods can also be used for this application. Moreover, simplicity, scalability, and robustness of the IMG models are the most important features, which should be focused on in future works.

5.2. In stability analysis

CB-IMGs are the most common structure of IMGs, which due to the weakness of such grids and low inertia, their voltage and frequency are very loose and hard to be controlled. Recently, powerful control methods have been proposed for these IMGs using distributed pinning

consensus-based secondary controllers. Hence, many previous stability analyses of CB-IMGs belong to poor control methods and/or even analytical not practical methods. Although an LT-based asymptotic stability proof is theoretically represented [45,46,72,76,79], small-signal stability is not assessed to recognize the impact of IMG power exchange controller parameters, and critical dynamic modes are not well identified. Delay-dependent stability analysis of ac IMGs [37] is less taken into account than that of dc IMGs, and can be extended for the communication-oriented control of such IMGs.

Despite the existing small-signal stability analyses for different IMG types, more analytical large-signal stability assessment methods are required to study various IMG operating points, e.g. equal-area criterion [148,160]. Synchronization process in CB-IMGs is more challenging than that of conventional multi-area power systems as well as that of grid-connected MGs/DERs. It is due to being very weak IMGs dislike strong multiple power systems in the second and the main wide grid in the third. Hence, the synchronization stability of CB-IMGs is an important issue to be studied.

Another gap is related to IMG elements analysis. Droop-based grid-forming DERs as the most important control actuators are taken into account. However, PQ-controlled grid-feeding [46] and virtual synchronous generator (VSG)-controlled grid-supporting [167] are well-known DER types, which should be considered in terms of IMG stability and control. Furthermore, possible improvement in IMG stability and inertia using VSG control methods either for DERs or for IL power controllers can be investigated. Different load types are another group of elements, which are not studied in IMG stability. Harmonic modeling and stability analysis [147] of power electronics-integrated IMGs are also necessary to be assessed.

5.3. In control field

Some ideas for future works in IMG control are given below.

- The control of CB-IMGs are more challenging due to direct interconnection by CBs. Therefore, it needs to be studied from different aspects, e.g. smooth synchronization and islanding controls.
- Although power exchange based on certain power references for BTBCs is possible in BTBC-IMGs, it has not been studied in CB-IMGs, and only power sharing among them based on the capacities, and frequency and voltage stability objectives have been addressed. However, sharing of IMG powers is not always an economic and desirable solution. Hence, power reference-based power exchange among CB-IMGs is a necessary control strategy to be investigated considering stability restrictions.
- Developing CB-IMG controllers to damp the inter-MG modes oscillations in an efficient way and using virtual impedance methods [185,186] to improve power sharing among IMGs.
- Studying inertial and transient responses of IMG frequency and investigating the role of VSG control in their enhancement.
- Rescheduling the MG load shedding control considering IMG power exchanges, which can postpone or even prevent in some cases the common load shedding algorithms.
- Analyzing Faults for ILs as well as studying fault ride-through capability [187] and low voltage ride-through capability [188] for BTBC converters in BTBC-IMGs.
- A detailed comparison between different control architectures of IMGs and their implementing methods like consensus protocol and MAS in order to obtain the optimized choice.
- Solving the communication delay challenge using advanced control methods, e.g. robust and predictive controllers. Already, integral and PI controllers are widely used, which can be replaced to gain a better performance.
- Introducing more objectives for deciding the power exchange among MGs and realizing the corresponding controllers like cyber security of control communication [189], resilience [190,

191], power quality [192], and using new data-driven control approaches like machine learning [193]. IMGs, as very weak grid systems, need to be more resilient against cyber–physical disasters and large-signal disturbances, and their modeling, stability, and control need to be reconsidered in both the primary and secondary control layers using resilient control approaches. In the primary control layer, the role of grid-forming power converters would be highlighted for more resilient power-angle stability. In addition, the role of a resilient cooperative secondary controller can become a more vital factor for avoiding the overall collapse of the system, where they are dramatically vulnerable to cyber-attack and threats.
- Optimization in communication-oriented controllers, e.g. using event/time-triggered methods to find a more reliable, less error, and cheaper performance.

6. Conclusion

After a comprehensive review on the research works in the fields of modeling, stability analysis and control of interconnected MGs, the literature has been organized in several classifications. For all the literatures, the IMG architecture, modeling type/method, model order level, simplification type/method, scalability level, stability analysis type/method, and important features of the stability assessment are determined. Moreover, control architecture/layer/type/design method, main control objective and designed controller validation method of the literature are specified to be easily followed by the potential users.

Detailed models are hard to be used for large-scale interconnected MGs. Simplified model-based, module-based, and measurement-based models should be much more considered based on applications, e.g. frequency control and stability or voltage regulation. The first group has been mostly used in the literature while the second has lower computational burdens and thus lower analysis times. Measurement-based and data-driven modeling and control methods can be of interest in future works due to their focus on the studied variable and existing required data communicated widely in smart grids.

Stability classification of islanded MGs is updated for interconnected MGs by focusing on inter-MG power balance and communication-related stability issues. Inter-MG dynamic modes and correlated oscillations, especially in CB-IMGs, have been recognized, which related control loops, generally in high control levels e.g. secondary level, should be enhanced to damp them. On the other hand, in BTBC-IMGs, dc link voltage of BTBCs leads to an independent frequency control of IMGs, which it expects to decrease power oscillations. However, dc links transmit such oscillations through dc voltages. Therefore, the challenge of power oscillations also exists in BTBC-IMGS, and BTBC dc voltage controllers should be improved in this regard.

Generally, a common CB-IMG control leads to power sharing usually using a pinning consensus protocol, while a common BTBC-IMG control results in exchanging certain power values among IMGs. BTBCs increase such a controllability to BTBC-IMGs with respect to CB-IMGs. This limitation can be eliminated and a power exchange objective can be followed by improving control functions. Control and stability challenges of weak CB-IMGs synchronization and communication-based challenges of all IMGs like cyber security have been less taken into account, which should be investigated in future works.

Declaration of competing interest

The authors declare the following financial interests/personal relationships which may be considered as potential competing interests: Frede Blaabjerg reports financial support was provided by Villum Foundation.

Data availability

Data will be made available on request.

References

[1] Bevrani H, François B, Ise T. Microgrid dynamics and control. John Wiley & Sons; 2017, Hoboken, NJ, USA.

[2] Lasseter RH. Smart distribution: Coupled microgrids. Proc IEEE 2011;99(6):1074–82.

[3] Shahidehpour M, Li Z, Bahramirad S, Li Z, Tian W. Networked microgrids: Exploring the possibilities of the IIT-bronzeville grid. IEEE Power Energy Mag 2017;15(4):63–71.

[4] Alam MN, Chakrabarti S, Ghosh A. Networked microgrids: State-of-the-art and future perspectives. IEEE Trans Ind Inf 2018;15(3):1238–50.

[5] Xu Z, et al. Analysis on the organization and Development of multi-microgrids. Renew Sustain Energy Rev 2018;81:2204–16.

[6] Bullich-Massagué E, et al. Microgrid clustering architectures. Appl Energy 2018;212:340–61.

[7] Nejabatkhah F, Li YW, Tian H. Power quality control of smart hybrid AC/DC microgrids: An overview. IEEE Access 2019;7:52295–318.

[8] Gupta A, Doolla S, Chatterjee K. Hybrid AC–DC microgrid: systematic evaluation of control strategies. IEEE Trans Smart Grid 2017;9(4):3830–43.

[9] Yu H, Niu S, Shang Y, Shao Z, Jia Y, Jian L. Electric vehicles integration and vehicle-to-grid operation in active distribution grids: A comprehensive review on power architectures, grid connection standards and typical applications. Renew Sustain Energy Rev 2022;168:112812.

[10] Savio DA, Juliet VA, Chokkalingam B, Padmanaban S, Holm-Nielsen JB, Blaabjerg F. Photovoltaic integrated hybrid microgrid structured electric vehicle charging station and its energy management approach. Energies 2019;12(1):168.

[11] Zhaoxia X, Tianli Z, Huaimin L, Guerrero JM, Su C-L, Vásquez JC. Coordinated control of a hybrid-electric-ferry shipboard microgrid. IEEE Trans Transp Electrif 2019;5(3):828–39.

[12] Ahmed M, Vahidnia A, Meegahapola L, Datta M. Small signal stability analysis of a hybrid AC/DC microgrid with static and dynamic loads. In: 2017 Australasian universities power eng. conf.. IEEE; 2017, p. 1–6.

[13] Ahmed M, Meegahapola L, Vahidnia A, Datta M. Analysis and mitigation of low-frequency oscillations in hybrid AC/DC microgrids with dynamic loads. IET Gen Transm Dist 2019;13(9):1477–88.

[14] Li Z, Shahidehpour M. Small-signal modeling and stability analysis of hybrid AC/DC microgrids. IEEE Trans Smart Grid 2017;10(2):2080–95.

[15] Ahmed M, Meegahapola L, Vahidnia A, Datta M. Stability and control aspects of microgrid architectures–A comprehensive review. IEEE Access 2020;8:144730–66.

[16] Malik SM, Ai X, Sun Y, Zhengqi C, Shupeng Z. Voltage and frequency control strategies of hybrid AC/DC microgrid: a review. IET Gen Transm Dist 2017;11(2):303–13.

[17] Sahoo SK, Sinha AK, Kishore N. Control techniques in AC, DC, and hybrid AC–DC microgrid: a review. IEEE J Emerg Sel Top Power Electron 2017;6(2):738–59.

[18] Zhang F, Jamalzadeh R, Hong M. A dynamic simulation study of networked microgrids in active distribution system. In: 2016 IEEE power & energy society innov. smart grid technol. conf.. IEEE; 2016, p. 1–5.

[19] Ambia MN, Meng K, Xiao W, Dong ZY. Comprehensive solution of networked microgrid towards enhanced overload resiliency. In: 2018 Int. conf. power syst. technol.. IEEE; 2018, p. 1736–42.

[20] Chowdhury AH, Asaduz-Zaman M. Load frequency control of multi-microgrid using energy storage system. In: 8th IEEE int. conf. electr. and computer eng.. 2014, p. 548–51.

[21] Gheisarnejad M, Khooban MH. Secondary load frequency control for multi-microgrids: HiL real-time simulation. Soft Comput 2019;23(14):5785–98.

[22] Tungadio DH, Bansal RC, Siti MW. Optimal control of active power of two micro-grids interconnected with two AC tie-lines. Electr Power Components Syst 2017;45(19):2188–99.

[23] Lal DK, Barisal AK, Tripathy M. Load frequency control of multi area interconnected microgrid power system using grasshopper optimization algorithm optimized fuzzy PID controller. In: 2018 Recent advances on eng., technol. and comput. sciences. IEEE; 2018, p. 1–6.

[24] Liu K, Liu T, Jill D. Frequency control in networked microgrids with voltage-sensitive loads. In: Proc. IREP symp.. 2017, p. 1–6.

[25] Dou C, Li Y, Yue D, Zhang Z, Zhang B. Distributed cooperative control method based on network topology optimisation in microgrid cluster. IET Ren Power Gen 2020;14(5):939–47.

[26] Akhavan A, Mohammadi HR, Vasquez JC, Guerrero JM. Coupling effect analysis and control for grid-connected multi-microgrid clusters. IET Power Electron 2020;13(5):1059–70.

[27] Veerashekar K, Eichner S, Luther M. Modelling and transient stability analysis of interconnected autonomous hybrid microgrids. In: 2019 IEEE Milan PowerTech. IEEE; 2019, p. 1–6.

[28] Goyal M, Ghosh A. Microgrids interconnection to support mutually during any contingency. Sustain Energy Grids Netw 2016;6:100–8.

[29] Nutkani IU, Loh PC, Blaabjerg F. Distributed operation of interlinked AC microgrids with dynamic active and reactive power tuning. IEEE Trans Ind Appl 2013;49(5):2188–96.

[30] Nutkani IU, Loh PC, Blaabjerg F. Power flow control of intertied AC microgrids. IET Power Electron 2013;6(7):1329–38.

[31] Nutkani IU, Loh PC, Wang P, Jet TK, Blaabjerg F. Intertied AC–AC microgrids with autonomous power import and export. Int J Electr Power Energy Syst 2015;65:385–93.

[32] Susanto J, Shahnia F, Ghosh A, Rajakaruna S. Interconnected microgrids via back-to-back converters for dynamic frequency support. In: IEEE power eng. conf.. Sep. 2014, p. 1–6.

[33] Khederzadeh M, Maleki H, Asgharian V. Frequency control improvement of two adjacent microgrids in autonomous mode using back to back Voltage-Sourced Converters. Int J Electr Power Energy Syst 2016;74:126–33.

[34] Bala S, Venkataramanan G. Autonomous power electronic interfaces between microgrids. In: 2009 IEEE energy conv. congress and exposition. IEEE; 2009, p. 3006–13.

[35] Aouini R, Marinescu B, Kilani KB, Elleuch M. Stability improvement of the interconnection of weak AC zones by synchronverter-based HVDC link. Elect Power Syst Res 2017;142:112–24.

[36] Pashajavid E, Ghosh A, Zare F. A multimode supervisory control scheme for coupling remote droop-regulated microgrids. IEEE Trans Smart Grid 2018;9(5):5381–92.

[37] Hao R, Ai Q, Jiang Z, Zhu Y. A novel adaptive control strategy of interconnected microgrids for delay-dependent stability enhancement. Int J Electr Power Energy Syst 2018;99:566–76.

[38] Naderi M, Khayat Y, Shafiee Q, Dragicevic T, Bevrani H, Blaabjerg F. Comprehensive small-signal modeling and Prony analysis-based validation of synchronous interconnected microgrids. Energy Rep 2021;7:6677–89.

[39] Huang T, Gao S, Xie L. Transient stability assessment of networked microgrids using neural Lyapunov methods. 2020, arXiv preprint arXiv:2012.01333.

[40] Madureira A, et al. Advanced control and management functionalities for multi-microgrids. Euro Trans Electr Power 2011;21(2):1159–77.

[41] Arefifar SA, Ordonez M, Mohamed YA-RI. Voltage and current controllability in multi-microgrid smart distribution systems. IEEE Trans Smart Grid 2016;9(2):817–26.

[42] Li Y, Qin Y, Zhang P, Herzberg A. SDN-enabled cyber-physical security in networked microgrids. IEEE Trans Sustain Energy 2018;10(3):1613–22.

[43] Toro V, Mojica-Nava E. Droop-free control for networked microgrids. In: 2016 IEEE conf. control appl.. IEEE; 2016, p. 374–9.

[44] Hirase Y, Ohara Y, Bevrani H. Virtual synchronous generator based frequency control in interconnected microgrids. Energy Rep 2020;6:97–103.

[45] Ren L, et al. Enabling resilient distributed power sharing in networked microgrids through software defined networking. Appl Energy 2018;210:1251–65.

[46] Liu W, Gu W, Xu Y, Wang Y, Zhang K. General distributed secondary control for multi-microgrids with both PQ-controlled and droop-controlled distributed generators. IET Gen Transm Dist 2017;11(3):707–18.

[47] Gil NJ, Lopes JP. Hierarchical frequency control scheme for islanded multi-microgrids operation. In: 2007 IEEE Lausanne power tech.. IEEE; 2007, p. 473–8.

[48] Schneider KP, et al. Improving primary frequency response to support networked microgrid operations. IEEE Trans Power Syst 2018;34(1):659–67.

[49] Ng EJ, El-Shatshat RA. Multi-microgrid control systems (MMCS). In: IEEE PES general meet.. IEEE; 2010, p. 1–6.

[50] Zhang F, Zhao H, Hong M. Operation of networked microgrids in a distribution system. CSEE J Power Energy Syst 2015;1(4):12–21.

[51] Zhang Y, Xie L, Ding Q. Interactive control of coupled microgrids for guaranteed system-wide small signal stability. IEEE Trans Smart Grid 2016;7(2):1088–96.

[52] Kavousi-Fard A, Wang M, Su W. Stochastic resilient post-hurricane power system recovery based on mobile emergency resources and reconfigurable networked microgrids. IEEE Access 2018;6:72311–26.

[53] Resende F, Gil NJ, Lopes JP. Service restoration on distribution systems using Multi-MicroGrids. Euro Trans Electr Power 2011;21(2):1327–42.

[54] Shahnia F, Chandrasena RP, Rajakaruna S, Ghosh A. Primary control level of parallel distributed energy resources converters in system of multiple interconnected autonomous microgrids within self-healing networks. IET Gen Transm Dist 2014;8(2):203–22.

[55] Sofla MA, King R. Control method for multi-microgrid systems in smart grid environment—Stability, optimization and smart demand participation. In: 2012 IEEE PES innov. smart grid technol.. IEEE; 2012, p. 1–5.

[56] Harmon E, et al. The internet of microgrids: A cloud-based framework for wide area networked microgrids. IEEE Trans Ind Inf 2017;14(3):1262–74.

[57] Wu X, Xu Y, Wu X, He J, Guerrero JM, Liu C-C, et al. A two-layer distributed control method for islanded networked microgrid systems. IEEE Trans Smart Grid 2019;11(2):942–57.

[58] Yuen C, Oudalov A, Timbus A. The provision of frequency control reserves from multiple microgrids. IEEE Trans Ind Electron 2010;58(1):173–83.

[59] Zhang Y, Xie L. A transient stability assessment framework in power electronic-interfaced distribution systems. IEEE Trans Power Syst 2016;31(6):5106–14.

[60] Golpîra H, Seifi H, Haghifam MR. Dynamic equivalencing of an active distribution network for large-scale power system frequency stability studies. IET Gen Transm Dist 2015;9(15):2245–54.

[61] Golpîra H, Seifi H, Messina AR, Haghifam M-R. Maximum penetration level of micro-grids in large-scale power systems: frequency stability viewpoint. IEEE Trans Power Syst 2016;31(6):5163–71.

[62] Shuai Z, Peng Y, Liu X, Li Z, Guerrero JM, Shen ZJ. Dynamic equivalent modeling for multi-microgrid based on structure preservation method. IEEE Trans Smart Grid 2018. http://dx.doi.org/10.1109/TSG.2018.2844107.

[63] Rivera S, Farid A, Youcef-Toumi K. A multi-agent system coordination approach for resilient self-healing operations in multiple microgrids. In: Industrial agents. Elsevier; 2015, p. 269–85.

[64] Zhao Z, Yang P, Wang Y, Xu Z, Guerrero JM. Dynamic characteristics analysis and stabilization of PV-based multiple microgrid clusters. IEEE Trans Smart Grid 2017;10(1):805–18.

[65] Li Y, Zhang P, Luh PB. Formal analysis of networked microgrids dynamics. IEEE Trans Power Syst 2018;33(3):3418–27.

[66] Tuffner FK, Radhakrishnan N, Tang Y, Schneider KP. Grid friendly appliance controllers to increase the dynamic stability of networked resiliency-based microgrids. In: 2018 IEEE/PES transm. and dist. conf. and exposition. IEEE; 2018, p. 1–5.

[67] Li Y, Zhang P, Yue M. Networked microgrid stability through distributed formal analysis. Appl Energy 2018;228:279–88.

[68] Nikolakakos IP, et al. Stability evaluation of interconnected multi-inverter microgrids through critical clusters. IEEE Trans Power Syst 2016;31(4):3060–72.

[69] Zhang Y, Xie L. Online dynamic security assessment of microgrid interconnections in smart distribution systems. IEEE Trans Power Syst 2014;30(6):3246–54.

[70] Naderi M, Shafiee Q, Blaabjerg F, Bevrani H. Low-frequency small-signal modeling of interconnected AC microgrids. IEEE Trans Power Syst 2020;1–11.

[71] Yang L, Hu Z, Xie S, Kong S, Lin W. Adjustable virtual inertia control of supercapacitors in PV-based AC microgrid cluster. Electr Power Syst Res 2019;173:71–85.

[72] Lai J, Lu X, Yu X, Monti A. Cluster-oriented distributed cooperative control for multiple AC microgrids. IEEE Trans Ind Inf 2019;15(11):5906–18.

[73] He J, Wu X, Wu X, Xu Y, Guerrero JM. Small-signal stability analysis and optimal parameters design of microgrid clusters. IEEE Access 2019;7:36896–909.

[74] Wu X, et al. Pinning-based hierarchical and distributed cooperative control for AC microgrid clusters. IEEE Trans Power Electron 2020;35(9):9867–87.

[75] Li Y, Meng K, Dong ZY. Distributed consensus control with event-triggered communication for multi-microgrid cluster. In: 2019 IEEE Milan PowerTech. IEEE; 2019, p. 1–6.

[76] Weng S, Xue Y, Luo J, Li Y. Distributed secondary control for islanded microgrids cluster based on hybrid-triggered mechanisms. Processes 2020;8(3):370.

[77] Jianna O, Shuo L, Weidong C, Min G. Modeling and analysis of microgrid cluster simulation based on RTDS. In: 2nd IEEE conf. energy internet and energy syst. integration. IEEE; 2018, p. 1–5.

[78] Shen Y, et al. Distributed cluster control for multi-microgrids using pinning-based group consensus of multi-agent system. In: 5th IEEE int. conf. cloud computing and intel. syst.. IEEE; 2018, p. 1077–80.

[79] Lu X, Lai J, Yu X. A novel secondary power management strategy for multiple AC microgrids with cluster-oriented two-layer cooperative framework. IEEE Trans Ind Inf 2020;17(2):1483–95.

[80] Li Q, Gao M, Lin H, Chen Z, Chen M. MAS-based distributed control method for multi-microgrids with high-penetration renewable energy. Energy 2019;171:284–95.

[81] Choobineh M, Silva-Ortiz D, Mohagheghi S. An automation scheme for emergency operation of a multi-microgrid industrial park. IEEE Trans Ind Appl 2018;54(6):6450–9.

[82] Wu P, Huang W, Tai N, Liang S. A novel design of architecture and control for multiple microgrids with hybrid AC/DC connection. Appl Energy 2018;210:1002–16.

[83] Zamora R, Srivastava AK. Multi-layer architecture for voltage and frequency control in networked microgrids. IEEE Trans Smart Grid 2018;9(3):2076–85.

[84] Yoo H-J, Nguyen T-T, Kim H-M. Multi-frequency control in a stand-alone multi-microgrid system using a back-to-back converter. Energies 2017;10(6):1–18.

[85] Majumder R, Bag G. Parallel operation of converter interfaced multiple microgrids. Int J Electr Power Energy Syst 2014;55:486–96.

[86] Naderi M, Khayat Y, Shafiee Q, Dragicevic T, Bevrani H, Blaabjerg F. Interconnected autonomous AC microgrids via back-to-back converters—Part I: small-signal modeling. IEEE Trans Power Electron 2019;35(5):4728–40.

[87] Naderi M, et al. Interconnected autonomous AC microgrids via back-to-back converters-Part II: Stability analysis. IEEE Trans Power Electron 2020;35(11):11801–12.

[88] Naderi M, Khayat Y, Shafiee Q, Dragicevic T, Blaabjerg F, Bevrani H. An emergency active and reactive power exchange solution for interconnected microgrids. IEEE J Emerg Sel Top Power Electron 2019;1–13.

[89] Naderi M, et al. Modeling and stability analysis of back-to-back converters in networked microgrids. In: 45th Conf. IEEE ind. electron. society. Vol. 1. IEEE; 2019, p. 3925–30.

[90] Naderi M, et al. Model validation of power electronics-based networked microgrids by prony analysis. In: 21st Euro. conf. power electron. and appl.. IEEE; 2019, p. 1–10.

[91] Ferdous S, Shahnia F, Shafiullah G. Power sharing and control strategy for microgrid clusters. In: 9th Int. conf. power and energy syst.. IEEE; 2019, p. 1–5.

[92] John B, Ghosh A, Goyal M, Zare F. A DC power exchange highway based power flow management for interconnected microgrid clusters. IEEE Syst J 2019;13(3):3347–57.

[93] Hossain MJ, Mahmud MA, Milano F, Bacha S, Hably A. Design of robust distributed control for interconnected microgrids. IEEE Trans Smart Grid 2016;7(6):2724–35.

[94] Golsorkhi MS, Hill DJ, Karshenas HR. Distributed voltage control and power management of networked microgrids. IEEE J Emerg Sel Top Power Electron 2018;6(4):1892–902.

[95] Shahnia F. Stability and eigenanalysis of a sustainable remote area microgrid with a transforming structure. Sustain Energy Grids Netw 2016;8:37–50.

[96] Shahnia F, Arefi A. Eigenanalysis-based small signal stability of the system of coupled sustainable microgrids. Int J Electr Power Energy Syst 2017;91:42–60.

[97] Batool M, Shahnia F, Islam SM. Multi-level supervisory emergency control for operation of remote area microgrid clusters. J Mod Power Syst Clean Energy 2019;7(5):1210–28.

[98] Zhou J, et al. Event-based distributed active power sharing control for interconnected AC and DC microgrids. IEEE Trans Smart Grid 2018;5(6):6815–28.

[99] Che L, Shahidehpour M, Alabdulwahab A, Al-Turki Y. Hierarchical coordination of a community microgrid with AC and DC microgrids. IEEE Trans Smart Grid 2015;6(6):3042–51.

[100] Wang Z, et al. Asynchronous distributed power control of multi-microgrid systems. IEEE Trans Control Netw Syst 2020.

[101] Zhou X, et al. A microgrid cluster structure and its autonomous coordination control strategy. Int J Electr Power Energy Syst 2018;100:69–80.

[102] Lei Q, et al. Coordinated control for medium voltage DC distribution centers with flexibly interlinked multiple microgrids. J Mod Power Syst Clean Energy 2019;7(3):599–611.

[103] Xia Y, Wei W, Yu M, Peng Y, Tang J. Decentralized multi-time scale power control for a hybrid AC/DC microgrid with multiple subgrids. IEEE Trans Power Electron 2017;33(5):4061–72.

[104] Guo L, Li P, Li X, Huang D, Zhu J. Flexible control of DC interlinked multiple MGs cluster. IET Gen Transm Dist 2018;13(11):2088–101.

[105] Ferdous S, Shahnia F, Shafiullah G. Stability and robustness of a coupled microgrid cluster formed by various coupling structures. Chinese J Electr Eng 2017;32(5):3704–14.

[106] Zolfaghari M, Abedi M, Gharehpetian GB. Power exchange control of clusters of multiple AC and DC microgrids interconnected by UIPC in hybrid microgrids. In: 2019 24th Electr. power dist. conf.. IEEE; 2019, p. 22–6.

[107] Nasir M, Jin Z, Khan HA, Zaffar NA, Vasquez JC, Guerrero JM. A decentralized control architecture applied to DC nanogrid clusters for rural electrification in developing regions. IEEE Trans Power Electron 2018;34(2):1773–85.

[108] Konar S, Ghosh A. Interconnection of islanded DC microgrids. In: 2015 IEEE PES Asia-pacific power and energy eng. conf.. IEEE; 2015, p. 1–5.

[109] Kumar M, Srivastava SC, Singh SN, Ramamoorty M. Development of a control strategy for interconnection of Islanded direct current microgrids. IET Ren Power Gen 2014;9(3):284–96.

[110] Vuyyuru U, Maiti S, Chakraborty C. Active power flow control between DC microgrids. IEEE Trans Smart Grid 2019;10(5):5712–23.

[111] Weaver WW, Robinett R, Parker GG, Wilson DG. Distributed control and energy storage requirements of networked DC microgrids. Control Eng Pract 2015;44:10–9.

[112] Shafiee Q, Dragičević T, Vasquez JC, Guerrero JM. Hierarchical control for multiple DC-microgrids clusters. IEEE Trans Energy Conv 2014;29(4):922–33.

[113] Dong C, et al. Time-delay stability switching boundary determination for DC microgrid clusters with the distributed control framework. Appl Energy 2018;228:189–204.

[114] Han Y, et al. Coordinated power control with virtual inertia for fuel cell-based DC microgrids cluster. Int J Hydrog Energy 2019;44(46):25207–20.

[115] Li Y, Dong P, Liu M, Yang G. A distributed coordination control based on finite-time consensus algorithm for a cluster of DC microgrids. IEEE Trans Power Syst 2018;34(3):2205–15.

[116] Mudaliyar S, Duggal B, Mishra S. Distributed tie-line power flow control of autonomous DC microgrid clusters. IEEE Trans Power Electron 2020;35(10):11250–66.

[117] Han R, Tucci M, Martinelli A, Guerrero JM, Ferrari-Trecate G. Stability analysis of primary plug-and-play and secondary leader-based controllers for DC microgrid clusters. IEEE Trans Power Syst 2018;34(3):1780–800.

[118] Sahoo S, Mishra S, Fazeli SM, Li F, Dragičević T. A distributed fixed-time secondary controller for DC microgrid clusters. IEEE Trans Energy Conv 2019;34(4):1997–2007.

[119] Liu S, Liu R, Zheng J, Liu X. Predictive function control in tertiary level for power flow management of DC microgrid clusters. Electron Lett 2020;56(13):675–6.

[120] Khan MTA, Chakrabortty A, Husain I, Cisneros R. Coordinated control of energy storage in networked microgrids under unpredicted load demands. In: 2019 American control conf.. IEEE; 2019, p. 1573–8.

[121] Wilson DG, Weaver WW, Robinett RD, Glover SF. Nonlinear power flow control design for networked AC/DC based microgrid systems. In: 2018 American control conf.. IEEE; 2018, p. 5698–705.

[122] Wilson DG, Robinett III RD, Weaver WW, Glover SF. Nonlinear power flow control for networked AC/DC microgrids. 2020, Google Patents, US Patent 10, 666, 054.

[123] Ma J, Zhu M, Cai X, Li YW. Configuration and operation of DC microgrid cluster linked through DC-DC converter. In: 2016 IEEE 11th conf. ind. electron. and appl.. IEEE; 2016, p. 2565–70.

[124] Majumder R. A hybrid microgrid with DC connection at back-to-back converters. IEEE Trans Smart Grid 2014;5(1):251–9.

[125] Sun T, Lu J, Li Z, Lubkeman DL, Lu N. Modeling combined heat and power systems for microgrid applications. IEEE Trans Smart Grid 2017;9(5):4172–80.

[126] Rocabert J, Luna A, Blaabjerg F, Rodriguez P. Control of power converters in AC microgrids. IEEE Trans Power Electron 2012;27(11):4734–49.

[127] Pogaku N, Prodanovic M, Green TC. Modeling, analysis and testing of autonomous operation of an inverter-based microgrid. IEEE Trans Power Electron 2007;22(2):613–25.

[128] Tuffner FK, Schneider KP, Hansen J, Elizondo MA. Modeling load dynamics to support resiliency-based operations in low-inertia microgrids. IEEE Trans Smart Grid 2018;10(3):2726–37.

[129] Mahmoud MS, Hussain SA, Abido MA. Modeling and control of microgrid: An overview. J Franklin Inst 2014;351(5):2822–59.

[130] Luo L, Dhople SV. Spatiotemporal model reduction of inverter-based islanded microgrids. IEEE Trans Energy Conv 2014;29(4):823–32.

[131] Mariani V, Vasca F, Vásquez JC, Guerrero JM. Model order reductions for stability analysis of islanded microgrids with droop control. IEEE Trans Ind Electron 2014;62(7):4344–54.

[132] Rasheduzzaman M, Mueller JA, Kimball JW. Reduced-order small-signal model of microgrid systems. IEEE Trans Sustain Energy 2015;6(4):1292–305.

[133] Vorobev P, Huang P-H, Al Hosani M, Kirtley JL, Turitsyn K. High-fidelity model order reduction for microgrids stability assessment. IEEE Trans Power Syst 2017;33(1):874–87.

[134] Nikolakakos IP, Zeineldin H, El-Moursi MS, Kirtley JL. Reduced-order model for inter-inverter oscillations in Islanded droop-controlled microgrids. IEEE Trans Smart Grid 2017;9(5):4953–63.

[135] Eskandari M, Savkin AV. A critical aspect of dynamic stability in autonomous microgrids: Interaction of droop controllers through the power network. IEEE Trans Ind Inf 2021. http://dx.doi.org/10.1109/TII.2021.3108568.

[136] Wang S, Liu Z, Liu J, Boroyevich D, Burgos R. Small-signal modeling and stability prediction of parallel droop-controlled inverters based on terminal characteristics of individual inverters. IEEE Trans Power Electron 2019;35(1):1045–63.

[137] Pulcherio M, Illindala MS, Choi J, Yedavalli RK. Robust microgrid clustering in a distribution system with inverter-based DERs. IEEE Trans Ind Appl 2018;54(5):5152–62.

[138] Guerrero JM, Vasquez JC, Matas J, De Vicuña LG, Castilla M. Hierarchical control of droop-controlled AC and DC microgrids—A general approach toward standardization. IEEE Trans Ind Electron 2011;58(1):158–72.

[139] Nasir M, Anees M, Khan HA, Guerrero JM. Dual-loop control strategy applied to the cluster of multiple nanogrids for rural electrification applications. IET Smart Grid 2019;2(3):327–35.

[140] Han Y, Ning X, Yang P, Xu L. Review of power sharing, voltage restoration and stabilization techniques in hierarchical controlled DC microgrids. IEEE Access 2019;7:149202–23.

[141] Dragičević T, Lu X, Vasquez JC, Guerrero JM. DC microgrids—Part II: A review of power architectures, applications, and standardization issues. IEEE Trans Power Electron 2015;31(5):3528–49.

[142] Shuai Z, et al. Microgrid stability: Classification and a review. Renew Sustain Energy Rev 2016;58:167–79.

[143] Fontenot H, Dong B. Modeling and control of building-integrated microgrids for optimal energy management–A review. Appl Energy 2019;254:113689.

[144] Xiong L, Liu X, Liu Y, Zhuo F. Modeling and stability issues of voltage-source converter dominated power systems: A review. CSEE J Power Energy Syst 2020;1–18.

[145] Han H, Hou X, Yang J, Wu J, Su M, Guerrero JM. Review of power sharing control strategies for islanding operation of AC microgrids. IEEE Trans Smart Grid 2015;7(1):200–15.

[146] Han Y, Li H, Shen P, Coelho EAA, Guerrero JM. Review of active and reactive power sharing strategies in hierarchical controlled microgrids. IEEE Trans Power Electron 2016;32(3):2427–51.

[147] Wang X, Blaabjerg F. Harmonic stability in power electronic-based power systems: Concept, modeling, and analysis. IEEE Trans Smart Grid 2018;10(3):2858–70.

[148] Wang X, Taul MG, Wu H, Liao Y, Blaabjerg F, Harnefors L. Grid-synchronization stability of converter-based resources—An overview. IEEE Open J Ind Appl 2020;1:115–34.

[149] Khayat Y, et al. On the secondary control architectures of AC microgrids: An overview. IEEE Trans Power Electron 2019;35(6):6482–500.

[150] Han Y, Zhang K, Li H, Coelho EAA, Guerrero JM. MAS-based distributed coordinated control and optimization in microgrid and microgrid clusters: A comprehensive overview. IEEE Trans Power Electron 2017;33(8):6488–508.

[151] Naderi M. Dynamic modeling and simulation of interconnected microgrids. Mendeley Data 2022;V1. http://dx.doi.org/10.17632/p5h576s247.1, https://data.mendeley.com/datasets/p5h576s247/1.

[152] Wang C, Yu H, Li P, Wu J, Ding C. Model order reduction for transient simulation of active distribution networks. IET Gen Transm Dist 2015;9(5):457–67.

[153] Monadi M, et al. Measurement-based network clustering for active distribution systems. IEEE Trans Smart Grid 2019;10(6):6714–23.

[154] Yazdani A, Iravani R. Hoboken, NJ, USA: Wiley Online Library; 2010.

[155] Zou C, Rao H, Xu S, Li Y, Li W, Chen J, et al. Analysis of resonance between a VSC-HVDC converter and the AC grid. IEEE Trans Power Electron 2018;33(12):10157–68.

[156] Jamshidi M. Large-scale systems: modeling, control, and fuzzy logic. Prentice-Hall, Inc. 1996.

[157] Adib A, Fateh F, Shadmand MB, Mirafzal B. A reduced-order technique for stability investigation of voltage source inverters. In: IEEE energy conv. cong. and exposition. 2018, p. 5351–6.

[158] Naderi M, Khayat Y, Shafiee Q, Bevrani H. Modeling of voltage source converters in microgrids using equivalent thevenin circuit. In: 2018 9th Annual power electron., drives syst. and technol. conf.. IEEE; 2018, p. 510–5.

[159] Naderi M, Khayat Y, Shafiee Q, Bevrani H, Blaabjerg F. Modeling of Islanded microgrids using static and dynamic equivalent thevenin circuits. In: 2018 20th IEEE euro. conf. on power electron. and appl.. 2018, p. 1–10.

[160] Farrokhabadi M, Cañizares CA, Simpson-Porco JW, Nasr E, Fan L, Mendoza-Araya PA, et al. Microgrid stability definitions, analysis, and examples. IEEE Trans Power Syst 2019;35(1):13–29.

[161] Rodriguez-Cabero A, Roldán-Pérez J, Prodanovic M, Suul JA, D'Arco S. Coupling of AC grids via VSC-HVDC interconnections for oscillation damping based on differential and common power control. IEEE Trans Power Electron 2019;35(6):6548–58.

[162] Pavella M, Ernst D, Ruiz-Vega D. Transient stability of power systems: A unified approach to assessment and control. Springer Science & Business Media; 2012.

[163] Khan AZ, Shahzad F. A PC based software package for the equal area criterion of power system transient stability. IEEE Trans Power Syst 1998;13(1):21–6.

[164] James J, Hill DJ, Lam AY, Gu J, Li VO. Intelligent time-adaptive transient stability assessment system. IEEE Trans Power Syst 2018;33(1):1049–58.

[165] Pilotto L, Szechtman M, Hammad A. Transient AC voltage related phenomena for HVDC schemes connected to weak AC systems. IEEE Trans Power Deliv 1992;7(3):1396–404.

[166] Alaboudy AK, Zeineldin HH, Kirtley J. Microgrid stability characterization subsequent to fault-triggered islanding incidents. IEEE Trans Power Deliv 2012;27(2):658–69.

[167] Karimi A, Khayat Y, Naderi M, Dragičević T, Mirzaei R, Blaabjerg F, et al. Inertia response improvement in AC microgrids: A fuzzy-based virtual synchronous generator control. IEEE Trans Power Electron 2019;35(4):4321–31.

[168] Hou X, et al. Distributed hierarchical control of AC microgrid operating in grid-connected, islanded and their transition modes. IEEE Access 2018;6:77388–401.

[169] Huang Q, Vittal V. Integrated transmission and distribution system power flow and dynamic simulation using mixed three-sequence/three-phase modeling. IEEE Trans Power Syst 2017;32(5):3704–14.

[170] Bevrani H, Watanabe M, Mitani Y. Power system monitoring and control. John Wiley & Sons; 2014.

[171] Bevrani H. Robust power system frequency control. Springer; Springer, 2014.

[172] TP462 F. Identification of electromechanical modes in power systems. IEEE Task Force Rep 2012. http://dx.doi.org/10.1109/TPWRS.2015.2403290.

[173] Sauer PW, Pai MA, Chow JH. Power system dynamics and stability: with synchrophasor measurement and power system toolbox. John Wiley & Sons; 2017.

[174] Kontis EO, Papadopoulos TA, Chrysochos AI, Papagiannis GK. Measurement-based dynamic load modeling using the vector fitting technique. IEEE Trans Power Syst 2017;33(1):338–51.

[175] Lu C. Wavelet fuzzy neural networks for identification and predictive control of dynamic systems. IEEE Trans Ind Electron 2010;58(7):3046–58.

[176] Kontis EO, Papadopoulos TA, Syed MH, Guillo-Sansano E, Burt GM, Papagiannis GK. Artificial-intelligence method for the derivation of generic aggregated dynamic equivalent models. IEEE Trans Power Syst 2019;34(4):2947–56.

[177] Wang W, Fang X, Cui H, Li F, Liu Y, Overbye TJ. Transmission-and-distribution dynamic co-simulation framework for distributed energy resource frequency response. IEEE Trans Smart Grid 2021.

[178] Huang Q, Vittal V. Advanced EMT and phasor-domain hybrid simulation with simulation mode switching capability for transmission and distribution systems. IEEE Trans Power Syst 2018;33(6):6298–308.

[179] Leonori S, Mascioli FMF, Rizzi A. Machine learning techniques for microgrid energy management system modelling and design 2019.

[180] Du Y, Li F. Intelligent multi-microgrid energy management based on deep neural network and model-free reinforcement learning. IEEE Trans Smart Grid 2019;11(2):1066–76.

[181] Mohamed MA, Hajjiah A, Alnowibet KA, Alrasheedi AF, Awwad EM, Muyeen S. A secured advanced management architecture in peer-to-peer energy trading for multi-microgrid in the stochastic environment. IEEE Access 2021;9:92083–100.

[182] Kanwal S, Khan B, Ali SM. Machine learning based weighted scheduling scheme for active power control of hybrid microgrid. Int J Electr Power Energy Syst 2021;125:106461.

[183] Carpintero Rentería M. Improved modelling of microgrid distributed energy resources with machine learning algorithms. 2021, https://doi.org/10.3390/en14030523.

[184] Chávarro-Barrera L, Pérez-Londoño S, Mora-Flórez J. An adaptive approach for dynamic load modeling in microgrids. IEEE Trans Smart Grid 2021;12(4):2834–43.

[185] Çelik D, Meral ME. A coordinated virtual impedance control scheme for three phase four leg inverters of electric vehicle to grid (V2G). Energy 2022;246:123354.

[186] Vijay A, Parth N, Doolla S, Chandorkar MC. An adaptive virtual impedance control for improving power sharing among inverters in islanded AC microgrids. IEEE Trans Smart Grid 2021;12(4):2991–3003.

[187] Çelik D, Meral ME. Multi-objective control scheme for operation of parallel inverter-based microgrids during asymmetrical grid faults. IET Ren Power Gen 2020;14(13):2487–98.

[188] Mahela OP, Gupta N, Khosravy M, Patel N. Comprehensive overview of low voltage ride through methods of grid integrated wind generator. IEEE Access 2019;7:99299–326.

[189] Ma S, Li Y, Du L, Wu J, Zhou Y, Zhang Y, et al. Programmable intrusion detection for distributed energy resources in cyber–physical networked microgrids. Appl Energy 2022;306:118056.

[190] Mishra DK, Ray PK, Li L, Zhang J, Hossain M, Mohanty A. Resilient control based frequency regulation scheme of isolated microgrids considering cyber attack and parameter uncertainties. Appl Energy 2022;306:118054.

[191] Deng C, Guo F, Wen C, Yue D, Wang Y. Distributed resilient secondary control for DC microgrids against heterogeneous communication delays and DoS attacks. IEEE Trans Ind Electron 2021. http://dx.doi.org/10.1109/TIE.2021.3120492.

[192] Keyvani-Boroujeni B, Fani B, Shahgholian G, Alhelou HH. Virtual impedance-based droop control scheme to avoid power quality and stability problems in VSI-dominated microgrids. IEEE Access 2021;9. http://dx.doi.org/10.1109/ACCESS.2021.3122800.

[193] Abianeh AJ, Wan Y, Ferdowsi F, Mijatovic N, Dragicevic T. Vulnerability identification and remediation of FDI attacks in islanded DC microgrids using multi-agent reinforcement learning. IEEE Trans Power Electron 2021. http://dx.doi.org/10.1109/TPEL.2021.3132028.